

1 **Identification of an antiviral component from the venom of the scorpion**  
2 ***Liocheles australasiae* using transcriptomic and mass spectrometric**  
3 **analyses**

4  
5 Masahiro Miyashita<sup>1\*</sup>, Naoya Mitani<sup>1</sup>, Atsushi Kitanaka<sup>1</sup>, Mao Yakio<sup>1</sup>, Ming Chen<sup>2</sup>,  
6 Sachiko Nishimoto<sup>3</sup>, Hironobu Uchiyama<sup>4</sup>, Masayuki Sue<sup>5</sup>, Hak Hotta<sup>2,3</sup>, Yoshiaki  
7 Nakagawa<sup>1</sup>, and Hisashi Miyagawa<sup>1</sup>

8 <sup>1</sup>Graduate School of Agriculture, Kyoto University, Kyoto 606-8502, Japan

9 <sup>2</sup>Graduate School of Health Sciences, Kobe University, Kobe 650-0047, Japan

10 <sup>3</sup>Faculty of Clinical Nutrition and Dietetics, Konan Women's University, Kobe 658-0001,  
11 Japan

12 <sup>4</sup>NODAI Genome Research Center, Tokyo University of Agriculture, Tokyo 156-8502,  
13 Japan

14 <sup>5</sup>Department of Agricultural Chemistry, Tokyo University of Agriculture, Tokyo 156-  
15 8502, Japan

16 \*Corresponding author: e-mail; miyashita.masahiro.6e@kyoto-u.ac.jp

17 Postal address; Kitashirakawa Oiwakecho Sakyo-ku, Kyoto 606-8502, Japan

18  
19  
20 **Abstract**

21 Scorpion venom contains a variety of biologically active peptides. Among them,  
22 neurotoxins are major components in the venom, but it also contains peptides that show  
23 antimicrobial activity. Previously, we identified three insecticidal peptides from the  
24 venom of the *Liocheles australasiae* scorpion, but activities and structures of other venom  
25 components remained unknown. In this study, we performed a transcriptome analysis of  
26 the venom gland of the scorpion *L. australasiae* to gain a comprehensive understanding  
27 of its venom components. The result shows that potassium channel toxin-like peptides  
28 were the most diverse, whereas only a limited number of sodium channel toxin-like  
29 peptides were observed. In addition to these neurotoxin-like peptides, many non-

30 disulfide-bridged peptides were identified, suggesting that these components have some  
31 critical roles in the *L. australasiae* venom. In this study, we also isolated a component  
32 with antiviral activity against hepatitis C virus using a bioassay-guided fractionation  
33 approach. By integrating mass spectrometric and transcriptomic data, we successfully  
34 identified LaPLA<sub>2</sub>-1 as an anti-HCV component. LaPLA<sub>2</sub>-1 is a phospholipase A<sub>2</sub> having  
35 a heterodimeric structure that is N-glycosylated at the N-terminal region. Since the  
36 antiviral activity of LaPLA<sub>2</sub>-1 was inhibited by a PLA<sub>2</sub> inhibitor, the enzymatic activity  
37 of LaPLA<sub>2</sub>-1 is likely to be involved in its antiviral activity.

38

39 **Keywords**

40 bioactive peptide; glycosylation; hepatitis C; phospholipase; venom gland

41

42

43

## 44 **1. Introduction**

45 Scorpions use their venom to capture their prey and defend themselves against  
46 predators. For this purpose, scorpion venom is composed of a variety of biologically  
47 active peptides (Ahmadi et al., 2020). Among them, neurotoxins are the most effective  
48 components in capturing their prey, such as insects. These toxins can immediately stop  
49 the movement of prey by acting on their ion channels (Schwartz et al., 2012, Smith, J. J.  
50 et al., 2013). In addition, these neurotoxins often show selective toxicity between insects  
51 and mammals, which is conferred at the ion channel level (Gordon et al., 2007, Housley  
52 et al., 2017).

53 Scorpion toxins acting on ion channels are peptides cross-linked with multiple  
54 disulfide bonds (Quintero-Hernandez et al., 2013). These peptides can be classified into  
55 two groups based on their molecular size. The long-chain group consists of peptides with  
56 60-80 amino acid residues, which include toxins that act on Na<sup>+</sup> channels. The short-chain  
57 group consists of peptides with 20-50 amino acid residues, which include toxins that act  
58 on K<sup>+</sup>, Ca<sup>2+</sup>, and Cl<sup>-</sup> channels. The scorpion venom also contains many peptides without  
59 disulfide bonds. Most of these peptides show antimicrobial activity (Almaaytah and  
60 Albalas, 2014), some of which also exhibit insecticidal activity and/or synergistically  
61 enhance the activity of other toxins (Miyashita et al., 2010, Wullschleger et al., 2005). In  
62 addition to peptides, enzyme proteins are present in the scorpion venom, although their  
63 contribution to the biological activity of the venom remains unclear (Smith, J.J. and  
64 Alewood, 2015). Because of these diverse components, scorpion venom has been studied  
65 as a rich source of bioactive molecules, which provide useful information for the  
66 development of novel pesticides and drugs (Ghosh et al., 2019, Smith, J. J., et al., 2013).  
67 Scorpion toxins can also serve as an important probe for the study of ion channels (Herzig  
68 et al., 2020, Zhao, Y. et al., 2019).

69 Traditionally, the search for bioactive peptides/proteins has been conducted mainly  
70 relying on the bioassay-guided isolation procedure, in which high performance liquid  
71 chromatography (HPLC) fractionation and bioassay is repeated until a single active

72 component is obtained (Vetter et al., 2011). This approach has led to the discovery of a  
73 number of novel bioactive molecules with unique structures. However, it is often difficult  
74 to identify minor components in the venom using this approach. In such cases, cDNAs  
75 obtained by reverse transcription of the mRNAs in the venom gland have been amplified  
76 by polymerase chain reaction (PCR) using a primer constructed based on a partial  
77 sequence to determine the entire structure (Quintero-Hernandez et al., 2011). Recently,  
78 the advent of next-generation high-throughput sequencing technologies allows us to  
79 obtain sequences of all mRNAs expressed in the venom gland (transcriptome), which  
80 provides a comprehensive understanding of structures of venom components (Oldrati et  
81 al., 2016). Furthermore, the combination of transcriptome analysis with proteome  
82 analysis has accelerated the determination of mature structures of each component in the  
83 venom (Fu et al., 2018, Walker et al., 2020). Although bioactive components can be  
84 estimated based on their structural similarity with reported molecules using this  
85 approach, biological functions of many components remain unclear due to the absence of  
86 similar molecules reported. In this regard, the classical bioassay-guided approach is still  
87 effective for the discovery of bioactive components with unique structural characteristics,  
88 and its combination with transcriptome analysis should accelerate the structural  
89 determination.

90 It is known that infection with hepatitis C virus (HCV) often causes liver disease,  
91 including cirrhosis and hepatocellular carcinoma. Although highly effective direct-acting  
92 antivirals can cure the vast majority of HCV infections, in the absence of a vaccine, there  
93 is a continued demand for antiviral drugs against HCV. Of the various enemies and  
94 pathogens scorpions cope with, virus represents one of major threats, and actually the  
95 scorpion venom contains antiviral components to prevent infection via venom glands (da  
96 Mata et al., 2017, El-Bitar et al., 2015, Yacoub et al., 2020). In this context, the scorpion  
97 venom has been studied as one of the promising sources of antiviral molecules. Previously,  
98 we identified three insecticidal peptides from the venom of the *Liocheles australasiae*  
99 scorpion based on toxicity against insects (Juichi et al., 2019, Matsushita et al., 2009,

100 Matsushita et al., 2007). However, the venom has not been evaluated for other biological  
101 activities, including antiviral effects. Thus, in this study, we first performed a  
102 transcriptome analysis of the venom gland of *L. australasiae* to gain a comprehensive  
103 understanding of its venom components. Using this information coupled with the  
104 bioassay-guided approach, we identified a new component with antiviral activity against  
105 HCV from the venom of *L. australasiae*.

106

## 107 **2. Materials and methods**

### 108 *2.1. Biological materials*

109 The scorpions *L. australasiae* were collected in Ishigaki Island, located at the southern  
110 end of the Ryukyu Islands in Japan. They were reared in the laboratory under humid  
111 conditions at 25°C and fed crickets. The venom was obtained by mechanical stimulation  
112 as previously reported (Miyashita et al., 2007). The venom secreted on Parafilm was  
113 dissolved in aqueous 2% acetic acid and filtered, which was lyophilized and stored at –  
114 80°C.

115

### 116 *2.2. RNA extraction and sequencing*

117 The telsons were dissected from six specimens anesthetized on ice and placed in a  
118 glass tube of a micro tissue grinder. The total RNA was extracted using RNAiso Plus  
119 (Takara Bio, Kusatsu, Japan) and further purified using the RNeasy Mini Kit (Qiagen,  
120 Venlo, The Netherlands) according to the manufacturer's instructions. The integrity of the  
121 RNA was verified using a Bioanalyzer 2100 (Agilent Technologies, Santa Clara, CA,  
122 USA). The mRNA was isolated using the NEBNext Poly(A) mRNA Magnetic Isolation  
123 Module (New England Biolabs, Ipswich, MA, USA). A cDNA library was prepared from  
124 the purified mRNA using the NEBNext Ultra RNA Library Prep Kit for Illumina (New  
125 England Biolabs). The 100 bp paired-end sequencing was performed on an Illumina  
126 HiSeq2500 platform (San Diego, CA, USA). The short-read data were deposited to the  
127 Read Archive of DDBJ (accession number DRA010798).

128

### 129 *2.3. De novo assembly and functional annotations*

130 After adapter- and quality-trimming using the software TagDust (Lassmann et al.,  
131 2009) and Fastx-Toolkit ([http://hannonlab.cshl.edu/fastx\\_toolkit](http://hannonlab.cshl.edu/fastx_toolkit)), the cleaned reads were  
132 assembled into contigs with Trinity (2.06) (Haas et al., 2013) and Bridger (r2014-12-01)  
133 (Chang et al., 2015) software using the standard protocol. Coding regions were predicted  
134 by TransDecoder (2.0). The predicted sequences obtained using two different assembly  
135 software were separately submitted to similarity searches using the BLASTP program  
136 against a database containing only sequences identified from scorpion venom (the  
137 UniProt Animal Toxin Annotation Project) to annotate the functions of identified peptides  
138 and proteins through the local BLAST tool (Altschul et al., 1990). Coding regions of each  
139 component were further inspected and corrected manually by comparing them with the  
140 reported sequences. Multiple sequence alignments were performed using MAFFT online  
141 (Kato et al., 2019) and Clustal Omega (Madeira et al., 2019).

142

### 143 *2.4. HPLC purification*

144 The crude venom dissolved in distilled water was applied to a C4 semi-preparative  
145 column (10 × 250 mm, Grace Vydac, Deerfield, IL, USA). The column was eluted with  
146 0.1% trifluoro acetic acid (TFA) in water (solvent A) and 0.08% TFA in acetonitrile  
147 (solvent B) at a flow rate of 2 mL/min, using a linear gradient of 5–60% of solvent B over  
148 55 min. Elution was monitored by the UV absorbance at 215 nm. Fractions were collected  
149 every 5 min during gradient elution. Each fraction was submitted to the antiviral activity  
150 test after lyophilization, and the fraction showing activity was then applied to a C18  
151 microbore column (1.0 × 250 mm, Grace Vydac). The column was eluted with solvent A  
152 and B at a flow rate of 0.05 mL/min, using a linear gradient of 20–50% of solvent B over  
153 60 min. Each HPLC peak was individually collected and lyophilized. The most active  
154 fraction was further purified on the same C18 microbore column using a different solvent  
155 system. The column was eluted with 0.1% formic acid in water (solvent C) and 0.1%

156 formic acid in acetonitrile (solvent D) at a flow rate of 0.05 mL/min using a linear gradient  
157 of 5–55% solvent D over 50 min. The purity was checked by liquid chromatography/mass  
158 spectrometry (LC/MS) analysis as described below.

159

#### 160 *2.5. Mass spectrometric analysis*

161 LC/MS and LC/MS/MS measurements were carried out in a positive ion mode on an  
162 LCMS-IT-TOF mass spectrometer (Shimadzu, Kyoto, Japan) equipped with an  
163 electrospray ion source. Precursor ions were manually selected, and a collision-induced  
164 dissociation (CID) spectrum was obtained by using argon as a collision gas. Reversed-  
165 phase (RP)-HPLC separation was performed on a C18 microbore column (TSKgel ODS-  
166 100V 3  $\mu$ m, 1.0  $\times$  150 mm, Tosoh, Tokyo, Japan). The column was eluted with solvent C  
167 and solvent D at a flow rate of 0.05 mL/min, using a linear gradient of 5–70% of solvent  
168 D over 65 min. The mass scale was calibrated externally using sodium trifluoroacetate  
169 cluster ions.

170

#### 171 *2.6. Enzymatic digestion*

172 The protein was dissolved in a buffer containing 0.2 M Tris-HCl (pH 8.5), 6 M  
173 guanidine hydrochloride and 10 mM dithiothreitol (DTT), and the mixture was incubated  
174 at 50°C for 1 h. The reaction mixture was then mixed with iodoacetic acid (20 mM final  
175 concentration) and incubated at 28°C for 1 h. The solution was diluted three-fold with  
176 water, and the Cys-alkylated protein was digested with endoproteinase Lys-C (FUJIFILM  
177 Wako Pure Chemical Corporation, Osaka, Japan) or Glu-C (FUJIFILM Wako Pure  
178 Chemical Corporation) at 37 °C for 18 h at a peptide/enzyme ratio of 20:1 (w/w).

179

#### 180 *2.7. Deglycosylation*

181 The protein was dissolved in a solution containing 0.5% SDS and 40 mM DTT, and  
182 the mixture was incubated at 100°C for 10 min. The solution was diluted two-fold with a  
183 buffer containing 50 mM sodium acetate and 1% NP-20, then mixed with 5 units of

184 PNGase A (New England Biolabs, Ipswich, MA, USA) at 37°C for 1 h.

185

## 186 *2.8. Cell culture and viruses*

187 Huh7it-1 cells were cultivated in Dulbecco's modified Eagle's medium (FUJIFILM  
188 Wako Pure Chemical Corporation, Osaka, Japan) supplemented with fetal bovine serum  
189 (Biowest, Nuaille, France), non-essential amino acids (Thermo Fisher Scientific,  
190 Waltham, MA, USA), penicillin (100 IU/ml) and streptomycin (100 µg/ml) (Thermo  
191 Fisher Scientific). Cells were grown at 37°C in a 5% CO<sub>2</sub> incubator. The J6/JFH1-P47  
192 strain of HCV (El-Bitar, et al., 2015), the Trinidad 1751 strain of dengue virus (DENV)  
193 (El-Bitar, et al., 2015), the Nakayama strain of Japanese encephalitis virus (JEV) (Song  
194 et al., 1999), and the CHR3 strain of herpes simplex virus type 1 (HSV-1) (Aoki-Utsubo  
195 et al., 2018) prepared in Huh7it-1 cells were used in this study. Infectivity of the stock  
196 virus was  $1.5 \times 10^6$ ,  $9.0 \times 10^5$ ,  $5.0 \times 10^5$ , and  $2.0 \times 10^4$  cell-infecting units (CIU)/ml for  
197 HCV, DENV, JEV and HSV-1, respectively.

198

## 199 *2.9. Antiviral activity test*

200 Antiviral activity was tested according to two different experimental procedures as  
201 described below.

202 (i) Pretreatment of virus with venom components before and during virus inoculation  
203 (pretreatment). This procedure is used to determine virucidal (neutralizing) activity of a  
204 test sample (Aoki-Utsubo, et al., 2018, El-Bitar, et al., 2015). In brief, Huh7it-1 cells were  
205 seeded in 24-well plates ( $1.6 \times 10^5$  cells/well). A fixed amount of the virus (either 10-fold  
206 diluted or undiluted stock virus) was mixed with serial dilutions of the whole venom or  
207 separated HPLC fractions of the venom and inoculated to the cells for 2 h. The cells were  
208 then washed with medium to remove the residual virus and venom components, and  
209 further cultured in medium. Culture supernatants were obtained at 24–48 h post-infection  
210 and titrated for virus infectivity as described previously (El-Bitar, et al., 2015). After 24  
211 h, the virus-infected cells were washed with phosphate-buffered saline (PBS), fixed with



212 4% paraformaldehyde for 20 min, and permeabilized with 0.1% Triton X-100 in PBS for  
213 15 min at room temperature. After being washed three times with PBS, the cells were  
214 incubated with UV-inactivated HCV-infected patient's serum for 1 h, followed by  
215 incubation with FITC-conjugated goat anti-human IgG (Medical & Biological  
216 Laboratories Co., Ltd., Nagoya, Japan). The cells were counterstained with Hoechst  
217 33342 (Molecular Probes, Eugene, OR, USA) for 5 min, and HCV-infected cells were  
218 counted under a BX53LED-43FLD fluorescence microscope (Olympus Corporation,  
219 Tokyo, Japan). Virus and cells treated with medium served as controls. Percent inhibition  
220 of virus infectivity by the samples was calculated by comparing with the controls, and  
221 50% inhibitory concentrations (IC<sub>50</sub>) were determined. Experiments were performed in  
222 duplicate and repeated three times.

223 (ii) Treatment of virus-infected cells after virus has been entered the cells (post-entry  
224 treatment). This procedure is used to determine viral replication-inhibiting activity of a  
225 test sample in the infected cells (Aoki-Utsubo, et al., 2018, El-Bitar, et al., 2015) In brief,  
226 cells were inoculated with virus in the absence of the venom components for 2 h. The  
227 virus-infected cells were cultured in medium containing serial dilutions of the venom  
228 components. The virus-infected cells cultured in medium without the venom components  
229 served as a control. After 48 h, RNA was extracted from the cells and subjected to reverse  
230 transcription-quantitative PCR (RT-qPCR) as described below. Experiments were  
231 performed in duplicate and repeated three times.

232

### 233 *2.10. Reverse transcription-quantitative PCR (RT-qPCR)*

234 Total cellular RNA was extracted from the cells using NucleoSpin RNA extraction kit  
235 (TaKaRa Bio, Inc.) according to the manufacturer's instructions. RNA (1 µg) was reverse  
236 transcribed using a GoScript Reverse Transcription system (Promega) with random  
237 primers. The cDNA products were subjected to quantitative real-time PCR analysis using  
238 Power SYBR Green PCR Master kit (Thermo Fisher Scientific Corp.) and a StepOne  
239 qPCR system (Thermo Fisher). The primers used to amplify an NS5A region of the HCV

240 genome were 5'-AGACGTATTGAGGTCCATGC-3' (sense) and 5'-  
241 CCGCAGCGACGGTGCTGATAG-3' (antisense) (Deng, L. et al., 2011). As an internal  
242 control, human glyceraldehyde-3-phosphate dehydrogenase (GAPDH) gene expression  
243 levels were measured using primers 5'-GCCATCAATGACCCCTTCATT-3' (sense) and  
244 5' TCTCGCTCCTGGAAGATGG-3'. Relative quantity of HCV NS5A cDNA was  
245 calculated and expressed as an arbitrary unit for each sample.

246

### 247 *2.11. Cytotoxicity test*

248 Cytotoxicity of LaPLA<sub>2</sub>-1 was evaluated using the WST-1 reagent (Roche, Mannheim,  
249 Germany) as reported previously (El-Bitar, et al., 2015). Briefly, Huh7it-1 cells plated in  
250 each well of a 96-well plate (0.1 ml/well) were treated with serial dilutions (0.1 to 1,000  
251 ng/ml) of LaPLA<sub>2</sub>-1 at 37 °C for 24 h. Untreated cells served as a control. After this  
252 treatment, 10 µl of the WST-1 reagent was added to each well, and the cells were cultured  
253 for 4 h. The WST-1 reagent is converted to formazan by living cells. The amount of  
254 formazan, which correlates with the number of living cells, was determined by measuring  
255 the absorbance at 450 and 630 nm using a microplate reader. The percent cell viability  
256 compared to the untreated control was calculated, and the 50% cytotoxic concentration  
257 (CC<sub>50</sub>) was determined.

258

### 259 *2.12. Phospholipase A<sub>2</sub> activity test*

260 L- $\alpha$ -Phosphatidylcholine (from egg yolk, Nacalai Tesque, Kyoto, Japan) was  
261 suspended in a buffer containing 0.1 M Tris-HCl (pH 8.0), 10 mM CaCl<sub>2</sub>, and 0.2%  
262 TritonX-100 at a concentration of 2 mg/ml. The reaction was started with the addition of  
263 the PLA<sub>2</sub> solution to the buffer (total 100 µl) at 37°C. After incubation for 10 min at 37°C,  
264 the mixture was analyzed by LC/MS to quantitate the amount of 1-palmitoyl-*sn*-glycero-  
265 3-phosphocholine (P-lysoPC, *m/z* 540.3, [M+HCOOH-H]<sup>-</sup>) generated by the reaction.  
266 Conditions used for LC/MS analysis (LCMS-8030, Shimadzu) were as follows:  
267 ionization, ESI-negative; column, COSMOCORE 2.6C<sub>18</sub> (2.1×75 mm, Nacalai Tesque);

268 flow rate, 0.3 mL/min; mobile phase, solvent C and solvent D; gradient, 35–95% of  
269 solvent D over 30 min. The amount of P-lysoPC generated in the absence of  
270 phospholipase A<sub>2</sub> (PLA<sub>2</sub>) was subtracted from those generated in each experiment.  
271 Experiments were repeated three times. PLA<sub>2</sub> activity was expressed relative to that of  
272 PLA<sub>2</sub> from honeybee (*Apis mellifera*) venom (Sigma-Aldrich, St. Louis, MO, USA).

273

### 274 **3. Results**

#### 275 *3.1. Transcriptome analysis*

276 A total of 253,691,496 raw reads were obtained by sequencing. After adapter- and  
277 quality-trimming, the clean reads were assembled in a de novo fashion using Trinity,  
278 which resulted in 133,715 contigs with N50 of 849 bp (224–14,739 bp), and Bridger  
279 software, which resulted in 98,577 contigs with N50 of 1447 bp (201–21,016 bp).  
280 BLASTP search was performed for predicted coding regions against a database consisting  
281 of reported sequences identified from scorpion venom. This resulted in identification of  
282 77 transcripts encoding peptides and proteins similar to those of scorpion venom as shown  
283 in Fig. 1-5 and Table S1 and S2.

284

#### 285 *3.2. Components identified by venom gland transcriptome analysis*

##### 286 3.2.1. Non-disulfide bridged peptides

287 Scorpion venoms are rich in non-disulfide bridged peptides (NDBPs) (Almaaytah and  
288 Albalas, 2014). NDBPs are known to display diverse biological functions to defend from  
289 pathogen infection via the venom gland by showing antimicrobial activity and/or to  
290 capture prey by showing insecticidal activities (Almaaytah and Albalas, 2014, Dias et al.,  
291 2018, Miyashita, et al., 2010). NDBPs are classified into five subfamilies based on the  
292 sequence similarity and the molecular size. In this study, we identified nine transcripts  
293 coding for NDBPs (Fig. 2a); two transcripts (LaNDBP2-1 and LaNDBP2-2) sharing  
294 sequence similarity to those of group 2 consisting of long-chain multifunctional peptides,  
295 two transcripts (LaNDBP3-1 and LaNDBP3-2) to those of group 3 consisting of medium-

296 length antimicrobial peptides, and five transcripts (LaNDBP4-1, LaNDBP4-2,  
297 LaNDBP4-3, LaNDBP4-4, and LaNDBP4-5) to those of group 4 consisting of short  
298 antimicrobial peptides.

299

### 300 3.2.2. Invertebrate defensins

301 Defensins are cationic peptides stabilized with three disulfide bonds, which are  
302 observed in a wide variety of organisms, including plants, insects, and mammals (Holly  
303 et al., 2017, Yi et al., 2014). These peptides play an important role in innate immunity by  
304 showing antimicrobial activity. Peptides similar to defensins are also found in scorpion  
305 venom (Cheng et al., 2020, Harrison et al., 2014, Meng et al., 2016). Although a limited  
306 number of scorpion venom peptides were reported as a defensin, a similar structural motif  
307 exists in potassium channel toxins as described below (Zhu, S. Y. et al., 2014). In this  
308 study, we found three transcripts (LaDefensin1, LaDefensin2, and LaDefensin3) coding  
309 for invertebrate defensins, which share sequence similarity to AbDef-1 that was identified  
310 from the venom of *Androctonus bicolor* (Fig. 2b) (Zhang et al., 2015).

311

### 312 3.2.3. Potassium channel toxin-like peptides

313 Potassium channel toxins (KTx) are cysteine-rich peptides that act on potassium  
314 channels (Jimenez-Vargas et al., 2017). To date, a large number of KTx peptides have  
315 been identified from scorpion venom. KTx peptides are currently classified into seven  
316 groups ( $\alpha$ -,  $\beta$ -,  $\gamma$ -,  $\delta$ -,  $\epsilon$ -,  $\kappa$ -, and  $\lambda$ -KTx) based on the sequence similarity and disulfide-  
317 bonding patterns (Chen, Z. Y. et al., 2012, Jimenez-Vargas, et al., 2017). In this study, we  
318 identified 18 transcripts coding for KTx peptides, and the majority of them were  $\alpha$ -KTx  
319 peptides (La-alphaKTx1, La-alphaKTx2, La-alphaKTx3, La-alphaKTx4, La-alphaKTx5,  
320 La-alphaKTx6, La-alphaKTx7, La-alphaKTx8, and La-alphaKTx9, Fig. 3a).  $\alpha$ -KTx  
321 adopts a typical fold consisting of an  $\alpha$ -helix and three  $\beta$ -strands stabilized by three or  
322 four disulfide bonds (CS- $\alpha\beta$  fold). We also found three transcripts (La-betaKTx1, La-  
323 betaKTx2, and La-betaKTx3) coding for  $\beta$ -KTx peptides (Fig. 3b). These peptides adopt

324 a CS- $\alpha\beta$  fold as observed in  $\alpha$ -KTx peptides, but they have an additional  $\alpha$ -helical  
325 structure without disulfide bonds at the N-terminal region. La-betaKTx1 and La-  
326 betaKTx2 correspond to LaIT2 and LaIT3, which were previously identified from the *L.*  
327 *australasiae* venom at a peptide level, respectively (Juichi, et al., 2019, Matsushita, et al.,  
328 2009). Five transcripts (La-kappaKTx1, La-kappaKTx2, La-kappaKTx3, La-kappaKTx4,  
329 and La-kappaKTx5) coding for  $\kappa$ -KTx peptides were also found (Fig. 3c). Unlike  $\alpha$ - and  
330  $\beta$ -KTx peptides,  $\kappa$ -KTx peptides do not adopt a CS- $\alpha\beta$  fold, but instead they have two  
331 parallel  $\alpha$ -helices stabilized with two disulfide bonds. The inhibitory activity of  $\kappa$ -KTx  
332 on potassium channels is known to be relatively weak compared with that of  $\alpha$ -KTx  
333 peptides. Furthermore, one transcript (La-deltaKTx1) coding for  $\delta$ -KTx was identified,  
334 which has a similar structure with Kunitz-type protease inhibitors consisting of two  
335 antiparallel  $\beta$ -strands and an  $\alpha$ -helix stabilized by three or four disulfide bonds (Fig. 3d).  
336 Some  $\delta$ -KTx peptides, such as BmKTT-2 from the *Mesobuthus martensii* venom, are  
337 known to show inhibitory activity on both potassium channels and proteases (Chen, Z. Y.,  
338 et al., 2012).

339

#### 340 3.2.4. Disulfide-directed hairpin peptides

341 Peptides with disulfide-directed hairpin (DDH) motif were identified from the venom  
342 of the limited number of scorpion species (Horita et al., 2011, Smith, J. J. et al., 2011).  
343 Although DDH peptides contain only two disulfide bonds, their structures are similar to  
344 the inhibitory cystine knot (ICK) motif, which is stabilized by three disulfide bonds.  
345 LaIT1, an insecticidal peptide previously identified from the venom of *L. australasiae*, is  
346 the first example of DDH peptides (Matsushita, et al., 2007). In this study, two transcripts  
347 (LaDDH1 and LaDDH2) coding for DDH peptides were identified, in which LaDDH1  
348 corresponds to LaIT1 (Fig. 4a).

349

#### 350 3.2.5. Sodium channel toxin-like peptides

351 Sodium channel toxins (NaTxs) adopt a CS- $\alpha\beta$  fold as observed in  $\alpha$ -KTx peptides,

352 but their sequences are relatively long (58-76 residues) (Housley, et al., 2017, Quintero-  
353 Hernandez, et al., 2013). NaTx peptides were identified mainly from the venom of  
354 Buthidae scorpions, and their sodium channel modulating activity is thought to be  
355 responsible for the relatively high toxicity of Buthidae scorpion venom (Cid-Urbe et al.,  
356 2019, de Oliveira et al., 2015, Luna-Ramirez, K. et al., 2015, Ward et al., 2018, Zhao, R.  
357 M. et al., 2010, Zhong et al., 2017). In addition to ion channel modulating activity, several  
358 members of this family are known to induce adipocyte lipolysis by forming a homodimer  
359 (Soudani et al., 2005, Zhu, S. and Gao, 2006). In the present study, two transcripts  
360 (LaLAP1 and LaLAP2) coding for the peptides similar to lipolysis-activating peptides  
361 were identified (Fig. 4b). However, these peptides could have other biological functions  
362 because the total number or the position of Cys residues are different from those of the  
363 known lipolysis-activating peptides (Zhu, S. and Gao, 2006).

364

#### 365 3.2.6. Serine protease inhibitor-like peptides

366 Animal venom generally contains protease inhibitors probably for protecting the  
367 venom components from enzymatic degradation. Two types of inhibitors having different  
368 structural motifs (Kunitz- and Ascaris-type) are known to exist in scorpion venom (Chen,  
369 Z. Y. et al., 2013, Ranasinghe and McManus, 2013). In this study, we found one transcript  
370 (La-deltaKTx1) coding for Kunitz-type inhibitor-like peptides, which was classified as  $\delta$ -  
371 KTx peptides as described above (Fig. 3d). In addition, we found eight transcripts  
372 (LaAPI1, LaAPI2, LaAPI3, LaAPI4, LaAPI5, LaAPI6, LaAPI7, and LaAPI8) coding for  
373 Ascaris-type inhibitor-like peptides (Fig. 4c). Interestingly, LaAPI1 contains only eight  
374 Cys residues that can form four disulfide bonds, whereas a typical Ascaris-type motif is  
375 stabilized by five disulfide bonds.

376

#### 377 3.2.7. La1-like peptides

378 La1 was previously identified as the most abundant peptide in the *L. australasiae*  
379 venom (Miyashita, et al., 2007). To date, peptides similar to La1 have been identified

380 from the venom of diverse scorpion species, although their biological significance  
381 remains unknown. La1-like peptides adopt a single domain von Willebrand factor type C  
382 (SVWC) motif (Sheldon et al., 2007). Some peptides adopting this motif based on the  
383 position of Cys residues are classified as SVWC peptides. In the present study, we  
384 identified eight transcripts (La1, La1-1, La1-2, La1-3, La1-4, La1-5, La1-6, and La1-7)  
385 coding for La1-like or SVWC peptides (Fig. 5).

386

### 387 3.2.8. Enzymes

388 In scorpion venom, enzymes have not been recognized as major bioactive components.  
389 However, recent progress in venom gland transcriptome analysis revealed that there are  
390 various enzymes, such as phospholipase, metalloprotease, serine protease, and  
391 hyaluronidase, in the venom (Bordon et al., 2015, Carmo et al., 2014, Gao, R. et al., 2008,  
392 Krayem and Gargouri, 2020). In this study, we identified three transcripts (LaPLA<sub>2</sub>-1,  
393 LaPLA<sub>2</sub>-2, and LaPLA<sub>2</sub>-3) coding for phospholipase A<sub>2</sub>, and eight transcripts (LaSP1,  
394 LaSP2, LaSP3, LaSP4, LaSP5, LaSP6, LaSP7, and LaSP8) coding for serine protease  
395 (Table S2). In addition to these enzymes, we identified one transcript (La-alpha-amylase)  
396 coding for  $\alpha$ -amylase. Since only a limited number of  $\alpha$ -amylase sequences have been  
397 identified from scorpion venom at a transcript level, there is little information on their  
398 biological functions.

399

### 400 3.2.9. Other proteins

401 We identified 10 transcripts (LaCRVP1, LaCRVP2, LaCRVP3, LaCRVP4, LaCRVP5,  
402 LaCRVP6, LaCRVP7, LaCRVP8, LaCRVP9, and LaCRVP10) coding for cysteine-rich  
403 secretory proteins, and three transcripts (LaVP1, LaVP2, and LaVP3) coding for proteins  
404 with an insulin-like growth factor binding motif (Table S2). Although these proteins are  
405 widely observed in scorpion venom, their biological functions remain unknown (Amorim  
406 et al., 2019, de Oliveira, et al., 2015, Yang et al., 2014).

407

408 *3.3. Isolation of an anti-HCV component*

409 We first evaluated anti-HCV activity of the venom of *L. australasiae*. The result  
410 showed that the venom has a significant inhibitory activity against HCV infection at  
411 extremely low concentrations ( $IC_{50} = 0.01 \mu\text{g/ml}$ ). To isolate a component responsible for  
412 the anti-HCV activity, the venom was separated using RP-HPLC on a C4 column (Fig.  
413 6a). Each fraction was tested for anti-HCV activity, and the fraction eluting at 37-42 min  
414 was found to be active. This fraction was further separated using a C18 column (Fig. 6b).  
415 The HPLC peak eluting at 25.5-26.5 min showed the most significant activity, and the  
416 main component in this peak was found to be responsible for anti-HCV activity (Fig. 6c).  
417 Mass spectrometric analysis revealed the molecular mass of this component as 13,079.8  
418 Da.

419

420 *3.4. Structure determination of the anti-HCV component*

421 The anti-HCV component was subjected to reduction and alkylation reactions to  
422 examine the number of disulfide bonds in this molecule. LC/MS analysis showed that the  
423 molecule was separated into two parts after the reactions, indicating that the anti-HCV  
424 component consists of two subunits cross-linked with disulfide bonds (Fig. 7a).  
425 Molecular masses of each subunit after alkylation of Cys residues were determined as  
426 1145.2 Da (small subunit) and 12,524.7 Da (large subunit). A total increase of the  
427 molecular mass after Cys-alkylation was approximately 590 Da  $[(1145.2 + 12,524.7) -$   
428  $13,079.8 = 590.1]$ . Considering a mass shift due to carboxymethylation of Cys residues  
429 (118 Da per disulfide bond), we determined that the anti-HCV component contains five  
430 disulfide bonds ( $118 \times 5 = 590$ ).

431 To obtain partial sequence information from the anti-HCV component, MS/MS de  
432 novo sequencing analysis was performed for the small subunit. As shown in Fig. 7b, the  
433 sequence of the small subunit was determined as KCVAHWKES. This sequence was  
434 searched from all transcripts obtained in this study, and the anti-HCV component was  
435 identified as LaPLA<sub>2</sub>-1, one of the phospholipase A<sub>2</sub> proteins. As observed in other



436 scorpion PLA<sub>2</sub>s, LaPLA<sub>2</sub>-1 forms a heterodimeric structure through processing. However,  
437 a sequence region that corresponds to the large subunit could not be determined based on  
438 its observed molecular mass (12,524.7 Da). It was assumed that the large subunit  
439 undergoes some types of post-translational modifications (PTMs). To determine a mature  
440 structure of the large subunit of LaPLA<sub>2</sub>-1 including PTMs, it was digested with Lys-C  
441 or Glu-C, which was analyzed by LC/MS (Table 1). The N- and C-terminal sites of the  
442 large subunit were identified based on the sequences of two Lys-C digests (LIFPGTK and  
443 CFVLDCD), because these peptides cannot be generated by Lys-C digestion (–  
444 IHQR/LIFPG– and –VLDCD/KRRF–). The calculated molecular mass of the deduced  
445 sequence of the large subunit is 11,826.2 Da, which is still 698.5 Da lower than the  
446 measured value (12,524.7 Da). When the LC/MS data of Lys-C and Glu-C digests were  
447 carefully examined, the molecular masses of two digested peptides  
448 (AANYSDLGSAETDK and LIFPGTKWCGAGDKAANYSDLGSAE) were found  
449 to be 698 Da higher than those calculated without modifications. These peptides share the  
450 same sequence region containing an N-linked glycosylation consensus motif (NXS)  
451 (Marshall, 1972). This suggests that the Asn residue in this region is glycosylated. To  
452 confirm the existence of an N-linked glycan at this position, the protein was treated with  
453 PNGase A, which can cleave the N-glycan moiety from the Asn residue (Plummer and  
454 Tarentino, 1981). LC/MS analysis showed that the measured molecular mass of the large  
455 subunit after removal of N-glycan was identical to the calculated one (11,304.9 Da, Fig.  
456 S1). The large subunit without N-glycan was then treated with Lys-C after reduction and  
457 alkylation of Cys residues. The existence of the peptide containing an Asp residue instead  
458 of the N-glycosylated Asn residue was confirmed by LC/MS analysis (Table 1). To obtain  
459 structural information of the N-glycan moiety, MS/MS analysis was performed for the  
460 Lys-C digested peptide containing the N-glycan moiety. As shown in Fig. 8, several  
461 fragment ions formed through regular and successive losses of 203 and 145 Da, which  
462 correspond to an N-acetyl hexose and a deoxyhexose, respectively, were observed in the  
463 product ion spectrum. Based on the fragmentation pattern and the molecular masses, the

464 N-glycan moiety is supposed to consist of two N-acetyl hexoses and two deoxyhexoses.  
465 Considering the N-glycan structures and the biosynthetic pathways reported for  
466 arthropods including scorpions and insects (Hassani et al., 1999, Staudacher et al., 1992,  
467 Walski et al., 2017), the N-glycan structure in LaPLA<sub>2</sub>-1 was estimated as shown in Fig.  
468 8. Homology searches revealed that LaPLA<sub>2</sub>-1 shares high sequence similarity to  
469 hemilipin from *Hemiscorpius lepturus*, HgPLA<sub>2</sub> from *Hadrurus gertschi*, and  
470 phaiodactylipin from *Anuroctonus phaiodactylus* (Fig. 9) (Jridi et al., 2015, Schwartz et  
471 al., 2007, Valdez-Cruz et al., 2004).

472

### 473 3.5. Antiviral activity of LaPLA<sub>2</sub>-1

474 LaPLA<sub>2</sub>-1 inhibited infectivity of HCV in a concentration-dependent manner from 0.1  
475 to 100 ng/ml (Fig. 10). Antiviral activity of LaPLA<sub>2</sub>-1 against several viruses was further  
476 examined. Accordingly, IC<sub>50</sub> values of LaPLA<sub>2</sub>-1 against HCV, DENV and JEV, which  
477 belong to the family *Flaviviridae*, were 2.0, 3.4 and 5.7 ng/ml, respectively (Table 2). On  
478 the other hand, LaPLA<sub>2</sub>-1 did not exhibit virucidal activity against HSV-1, which belongs  
479 to the family *Herpesviridae* even at a much higher concentration (1,000 ng/ml) (Fig. 10  
480 and Table 2). To determine whether the post-entry step of the viral life cycle is affected  
481 by LaPLA<sub>2</sub>-1, possible effect of post-entry treatment with LaPLA<sub>2</sub>-1 on virus replication  
482 in infected cells was examined. The result demonstrated that post-entry treatment with  
483 LaPLA<sub>2</sub>-1 barely exhibited anti-HCV activity even at a high concentration (100 ng/ml),  
484 whereas pretreatment exhibited highly potent anti-HCV activity (Table S3).

485 To examine whether the virucidal activity of LaPLA<sub>2</sub>-1 against HCV is associated with  
486 its enzymatic activity, the effect of PLA<sub>2</sub> inhibitor on the anti-HCV activity was evaluated.  
487 The result obtained revealed a dramatic decrease of the virucidal activity in the presence  
488 of manoalide, the PLA<sub>2</sub> inhibitor (Lombardo and Dennis, 1985). In addition, LaPLA<sub>2</sub>-1  
489 exhibited the significant phospholipase activity at a comparable level that was observed  
490 for bee venom PLA<sub>2</sub> (Fig. 11). These results suggest that the virucidal activity of LaPLA<sub>2</sub>-  
491 1 against HCV is closely associated with its enzymatic activity. In the present study, the

492 concentration ranges of LaPLA<sub>2</sub>-1 that showed virucidal and PLA<sub>2</sub> activities appear to be  
493 different. However, this may be due to differences in states of the substrate (membrane  
494 versus solution) and incubation time used for measurements (2 h versus 10 min) between  
495 virucidal and PLA<sub>2</sub> activity tests.

496 We also evaluated the toxicity of LaPLA<sub>2</sub>-1 to the host cells. LaPLA<sub>2</sub>-1 showed no  
497 cytotoxic effect at concentrations of up to 100 ng/ml and only a marginal cytotoxic effect  
498 at 1,000 ng/ml (Table S4), suggesting that observed LaPLA<sub>2</sub>-1 action is specific to the  
499 viruses.

500

## 501 **4. Discussion**

### 502 *4.1. Peptides identified by venom gland transcriptome analysis*

503 Previously, we isolated and characterized four peptides (LaIT1, LaIT2, LaIT3, and  
504 La1) from the venom of the scorpion *L. australasiae*, mainly based on toxicity against  
505 insects (Juichi, et al., 2019, Matsushita, et al., 2009, Matsushita, et al., 2007, Miyashita,  
506 et al., 2007). In the present study, we performed the transcriptome analysis of the venom  
507 gland of *L. australasiae* to comprehensively understand the components in the venom.  
508 This resulted in the identification of 77 transcripts coding for peptides and proteins similar  
509 to those from the venom of other scorpion species. Among them, KTx-like peptides,  
510 including insecticidal toxins LaIT2 and LaIT3, were more diverse than other families of  
511 venom components (Fig. 1). On the other hand, only three NaTx-like peptides were  
512 identified in this study. This is consistent with the previous observations obtained by mass  
513 spectrometric analysis (Miyashita, et al., 2007). The number of the components with  
514 molecular masses of 6,000-9,000 Da, which may correspond to NaTx-like peptides,  
515 detected at the peptide level was relatively small in the *L. australasiae* venom when  
516 compared with that observed in the Buthidae scorpion venom. On the other hand, the  
517 number of the components with molecular masses of 3,000-5,000 Da, which may  
518 correspond to KTx-like peptides, was relatively large at the peptide level. A similar trend  
519 was noted in the transcriptome analysis of the venom glands of *Hadogenes troglodytes* of

520 the family Hormuridae (Zhong, et al., 2017). The study showed the existence of many  
521 KTx-like peptides in the venom, whereas no NaTx-like peptides were found. It is known  
522 that NaTx peptides have been found mainly from the venom of Buthidae scorpions (Cid-  
523 Uribe, et al., 2019, de Oliveira, et al., 2015, Luna-Ramirez, K., et al., 2015, Quintero-  
524 Hernandez, et al., 2013, Ward, et al., 2018, Zhao, R. M., et al., 2010, Zhong, et al., 2017).  
525 This suggests that sodium channels are not a main target of the venom components in  
526 non-Buthidae scorpions.

527 LaIT2 and LaIT3 belong to the  $\beta$ -KTx peptide group, which is structurally  
528 characterized by the  $\alpha$ -helical region attached to the N-terminal of a CS- $\alpha\beta$  fold. In  
529 addition to these toxins, we found another peptide having a structure similar to  $\beta$ -KTx  
530 peptides (Fig. 3b). This peptide (La-betaKTx3) has the sequence similar to scorpine-like  
531 peptides, such as SC11 from *Urodacus yaschenkoi*, which are classified as one of the  
532 subfamilies of  $\beta$ -KTx peptides (Luna-Ramirez, Karen et al., 2016, Luna-Ramirez, K. et  
533 al., 2013). Since scorpine-like peptides are known to show antibacterial activity, La-  
534 betaKTx3 is likely to have a similar biological function.

535 LaIT1 is the first insecticidal toxin identified from the *L. australasiae* venom  
536 (Matsushita, et al., 2007). In the present study, another peptide (LaDDH2) that has the  
537 sequence similar to LaIT1 was found (Fig. 4a). Two basic residues (R13 and R15) that  
538 are important for the expression of the insecticidal activity of LaIT1 are conserved in  
539 LaDDH2, suggesting that this peptide may also have insecticidal activity (Horita, et al.,  
540 2011). To date, peptides similar to LaIT1 have been identified from the family  
541 Hormuridae (*L. waigiensis* and *Opisthacanthus cayaporum*) (Silva et al., 2009, Smith, J.  
542 J., et al., 2011) and the family Hemiscorpiidae (*Hemiscorpius lepturus*) (Kazemi-  
543 Lomedasht et al., 2017). This suggests that LaIT1 and its related peptides have been  
544 evolved independently in limited scorpion species.

545 La1 was previously identified as the most abundant component in the *L. australasiae*  
546 venom, although its biological function remains unknown (Miyashita, et al., 2007).  
547 Unlike LaIT1, peptides similar to La1 have been found in a wide variety of scorpion

548 species from seven families; Buthidae (Zeng et al., 2013, Zhao, R. M., et al., 2010),  
549 Hemiscorpiidae (Kazemi-Lomedasht, et al., 2017), Hormuridae (Silva, et al., 2009,  
550 Zhong, et al., 2017), Scorpionidae (Abdel-Rahman et al., 2013, Deng, Y. C. et al., 2018,  
551 Diego-Garcia et al., 2012, Luna-Ramirez, K., et al., 2015), Superstitioniidae (Santibanez-  
552 Lopez et al., 2016), and Vaejovidae (Quintero-Hernandez et al., 2015, Romero-Gutierrez  
553 et al., 2018). Particularly, many La1-like peptides were observed in the venom gland  
554 transcriptome of *H. troglodytes* (Zhong, et al., 2017). Therefore, it is possible that La1-  
555 like peptides are abundant in the venom of Hormuridae scorpions, as observed in this  
556 study (Fig. 5). La1 adopts an SVWC motif, which has been observed in peptides from a  
557 wide variety of arthropods, including insects (Sheldon, et al., 2007). Recently, it has been  
558 reported that SVWC peptides may play a role in protection against entomopathogenic  
559 fungi in the epidermis of the silkworm and in basal AMPs expression of bumblebee (Han  
560 et al., 2017, Wang et al., 2017). Although the mechanisms of action of these peptides are  
561 still unknown, La1 might play a role in preventing pathogenic infections in the venom  
562 glands as well.

563 In addition to the peptides having disulfide bonds, many NDBPs were identified in  
564 this study (Fig. 2a). These peptides generally show membrane-disrupting activity by  
565 forming an amphipathic  $\alpha$ -helical structure (Harrison, et al., 2014). Among five  
566 subfamilies of scorpion NDBPs, peptides of four subfamilies were found in this study.  
567 The reasons for the presence of the various types of NDBPs in the venom are unknown,  
568 but they are likely to have different biological functions. For example, four NDBPs  
569 isolated from *Isometrus maculatus* show different antimicrobial spectra, and some of  
570 them also exhibit insecticidal and hemolytic activities (Miyashita et al., 2017).  
571 Furthermore, some NDBPs may have a synergistic effect on other neurotoxins in venom  
572 to enhance their activity (Gao, B. et al., 2018). Defensins are another type of antimicrobial  
573 peptides observed in a wide variety of organisms (Holly, et al., 2017, Yi, et al., 2014). In  
574 this study, three defensin-like peptides were found (Fig. 2b). Since invertebrate defensins  
575 have the same disulfide-bonding pattern as peptides that act on potassium channels, it is

576 also possible that defensins identified in this study could show some ion channel-  
577 modulating activity (Meng, et al., 2016).

578 A number of peptides similar to serine protease inhibitors were also found in the  
579 present study (Fig. 4c). Kunitz-type protease inhibitors have been found in many  
580 organisms (Mishra, 2020). The peptides having a Kunitz-type motif have been reported  
581 to be present in the venom of various scorpion species (Ranasinghe and McManus, 2013).  
582 In addition to Kunitz-type peptides, Ascaris-type protease inhibitors have also been  
583 identified from the scorpion venom (Chen, Z. Y., et al., 2013). These peptides are likely  
584 responsible for preventing degradation of venom components by proteases of its own or  
585 other organisms. In addition, some of the protease inhibitor peptides from scorpion venom  
586 are known to act on potassium channels. This is thought to be a result of divergent  
587 evolution. For example, BmKTT-2, a Kunitz-type peptide identified from *Mesobuthus*  
588 *martensii*, shows inhibitory activity on Kv1.3 channels as well as inhibition of trypsin  
589 activity (Chen, Z. Y., et al., 2012). Since La-deltaKTx1 identified in this study (Fig. 3d)  
590 shares sequence similarity to BmKTT-2, it could show potassium channel inhibition  
591 activity.

592

#### 593 4.2. Anti-HCV component in the *L. australasiae* venom

594 In the present study, we found that the *L. australasiae* venom has a potent virucidal  
595 activity against HCV and successfully identified LaPLA<sub>2</sub>-1 as an anti-HCV component  
596 in the venom using a bioassay-guided approach. PLA<sub>2</sub> enzymes can be found in a wide  
597 variety of organisms, including snake and bee venom (Dennis et al., 2011). They catalyze  
598 the hydrolysis of glycerophospholipids at the *sn*-2 position to release free fatty acids and  
599 lysophospholipids. PLA<sub>2</sub> molecules can be classified into six types, and scorpion venom  
600 PLA<sub>2</sub> (scvPLA<sub>2</sub>) belongs to group III of secreted PLA<sub>2</sub> (sPLA<sub>2</sub>) (Krayem and Gargouri,  
601 2020). This group also includes PLA<sub>2</sub> from bee venom (bvPLA<sub>2</sub>). Some of sPLA<sub>2</sub>  
602 molecules are known to exhibit antiviral activity, and their enzymatic activity is suggested  
603 to be associated with antiviral activity (Chen, M. et al., 2017). For example, PLA<sub>2</sub>

604 molecules from snake venom (svPLA<sub>2</sub>) specifically act on *Flaviviridae* viruses. This is  
605 likely because they can degrade the viral envelope membranes, particularly those derived  
606 from endoplasmic reticulum (ER). In fact, LaPLA<sub>2</sub>-1 efficiently inhibited the infection of  
607 *Flaviviridae* viruses such as HCV, DENV and JEV (IC<sub>50</sub> = 2.0, 3.4 and 5.7 ng/ml,  
608 respectively). A comparable degree of virucidal activity was reported for PLA<sub>2</sub>s obtained  
609 from snake venom (Teixeira et al., 2020). However, no significant antiviral activity was  
610 observed for a *Herpesviridae* virus such as HSV-1, which has the plasma membrane  
611 (PM)-derived envelope. This suggests that LaPLA<sub>2</sub>-1 has the same mechanism of action  
612 as svPLA<sub>2</sub> (Chen, M., et al., 2017). It has been shown that phaiodactylipin can hydrolyze  
613 phosphatidylcholine more preferably than phosphatidylethanolamine and  
614 phosphatidylserine (Valdez-Cruz, et al., 2004). Since the ER-budded viruses contain a  
615 relatively high proportion of phosphatidylcholine than PM-budded viruses (Callens et al.,  
616 2016), LaPLA<sub>2</sub> may have a similar substrate preference as observed for phaiodactylipin.  
617 The possible action specificity of LaPLA<sub>2</sub>-1 on the ER membrane implies that it may  
618 have no adverse effect on the host cells, which is further supported by its low cytotoxicity  
619 with CC<sub>50</sub> being >1,000 ng/ml. Although PLA<sub>2</sub>s, in general, are known to be cytotoxic  
620 and inflammatory or neurotoxic, LaPLA<sub>2</sub>-1 or its derivative(s) might be a good candidate  
621 as a lead compound for the development of an antiviral drug against HCV, DENV and  
622 other viruses budding from the ER membranes.

623 It is known that the Ca<sup>2+</sup>-binding motif (XCGXG) and the catalytic center with a His-  
624 Asp dyad are important for the expression of enzyme activity of PLA<sub>2</sub> (Dennis, et al.,  
625 2011). In the structures of scvPLA<sub>2</sub>s, these motifs are conserved except for  
626 phaiodactylipin, in which one of the Gly residues in the Ca<sup>2+</sup>-binding motif is missing  
627 (Fig. 9). The structure of scvPLA<sub>2</sub>s is further characterized by the formation of a  
628 heterodimer consisting of a large and a small subunit cross-linked with a disulfide bond,  
629 although its relevance to biological function remains unknown. It is also known that many  
630 bvPLA<sub>2</sub>s contain N-glycans, most of which are core-fucosylated (Kubelka et al., 1993).  
631 Glycosylation of scvPLA<sub>2</sub> molecules has been investigated particularly for

632 phaiodactylipin (Valdez-Cruz, et al., 2004). Three N-glycosylation sites were recognized  
633 in the structure of phaiodactylipin, one of which is located at the N-terminal region of the  
634 large subunit, as observed in LaPLA<sub>2</sub>-1 (Fig. 9). Hemilipin, HgPLA<sub>2</sub>, and bvPLA<sub>2</sub> also  
635 contain one or two possible N-glycosylation sites in their sequences, although the  
636 presence of glycans is not experimentally examined in hemilipin and HgPLA<sub>2</sub>. Among  
637 the N-glycosylation sites in these PLA<sub>2</sub> molecules, that at the N-terminal region of the  
638 large subunit is commonly observed. Since this site is close to the catalytic center, it may  
639 play an important role in enzymatic and/or antiviral activity.

640

## 641 **5. Conclusion**

642 Scorpion venom is known to be a rich source of bioactive peptides and proteins.  
643 Previously, we identified three insecticidal peptides from the venom of the *L. australasiae*  
644 scorpion, but the activities and structures of the other venom components remained  
645 unknown. In the present study, we performed a transcriptomic analysis of the venom  
646 gland of *L. australasiae* to elucidate a comprehensive picture of the venom components.  
647 As a result, 77 transcripts coding for venom peptides and proteins, including four  
648 previously reported peptides, were successfully identified. Among them, KTx-like  
649 peptides were the most diverse, suggesting that these peptides play a crucial role in this  
650 venom. On the other hand, a relatively small number of NaTx-like peptides were found.  
651 This is consistent with previous findings that NaTx-like peptides are predominantly found  
652 in the venom of Buthidae scorpions. In addition, a relatively large number of peptides  
653 without disulfide bonds were identified, suggesting that these peptides have some critical  
654 functions in the *L. australasiae* venom.

655 These transcriptome data facilitated the structural determination of the anti-HCV  
656 component in the venom, which was obtained by a bioassay-guided approach. Mass  
657 spectrometric analysis revealed that this component is one of the PLA<sub>2</sub>s (LaPLA<sub>2</sub>-1). This  
658 is the first report of a PLA<sub>2</sub> with antiviral activity from scorpion venom, although PLA<sub>2</sub>s  
659 from snake and bee venom are known to show antiviral activity. Since the anti-HCV



660 activity of LaPLA<sub>2</sub>-1 was inhibited by a PLA<sub>2</sub> inhibitor, the enzymatic activity of  
661 LaPLA<sub>2</sub>-1 is likely to be involved in its expression of the anti-HCV activity. It is known  
662 that scvPLA<sub>2</sub>s, including LaPLA<sub>2</sub>-1, adopt a heterodimeric structure and are likely to be  
663 post-translationally modified by N-glycosylation at the N-terminal region. Elucidation of  
664 the relationship between the characteristic structures and enzymatic/antiviral activity of  
665 scvPLA<sub>2</sub>s will be a subject of future research.

666

### 667 **Acknowledgements**

668 The authors are grateful to Dr. C. M. Rice (The Rockefeller University, New York, NY,  
669 U.S.A.) for providing pFL-J6/JFH1. We also thank Dr. Hajime Ono (Kyoto University)  
670 for valuable advice on the RNA extraction. This study was supported by the Cooperative  
671 Research Program of the Genome Research for BioResource, NODAI Genome Research  
672 Center, Tokyo University of Agriculture. This study was also supported in part by the  
673 Program on the Innovative Development and the Application of New Drugs for Hepatitis  
674 B from the Japan Agency for Medical Research and Development (AMED) under the  
675 grant number JP19fk0310103h2103 and by JSPS KAKENHI grant number JP19K05842.

676

677

### 678 **References**

- 679 Abdel-Rahman, M.A., Quintero-Hernandez, V., Possani, L.D., 2013. Venom proteomic  
680 and venomous glands transcriptomic analysis of the Egyptian scorpion *Scorpio*  
681 *maurus palmatus* (Arachnida: Scorpionidae). *Toxicon* 74, 193-207,  
682 10.1016/j.toxicon.2013.08.064
- 683 Ahmadi, S., Knerr, J.M., Argemi, L., Bordon, K.C.F., Pucca, M.B., Cerni, F.A., Arantes,  
684 E.C., Caliskan, F., Laustsen, A.H., 2020. Scorpion venom: Detriments and benefits.  
685 *Biomedicines* 8, 118, 10.3390/biomedicines8050118
- 686 Almaaytah, A., Albalas, Q., 2014. Scorpion venom peptides with no disulfide bridges: A  
687 review. *Peptides* 51, 35-45, 10.1016/J.Peptides.2013.10.021

688 Altschul, S.F., Gish, W., Miller, W., Myers, E.W., Lipman, D.J., 1990. Basic local  
689 alignment search tool. *J. Mol. Biol.* 215, 403-410, 10.1006/jmbi.1990.9999

690 Amorim, F.G., Longhim, H.T., Cologna, C.T., Degueldre, M., De Pauw, E., Quinton, L.,  
691 Arantes, E.C., 2019. Proteome of fraction from *Tityus serrulatus* venom reveals new  
692 enzymes and toxins. *J. Venom Anim. Toxins* 25, e148218, 10.1590/1678-9199-  
693 JVATITD-1482-18

694 Aoki-Utsubo, C., Chen, M., Hotta, H., 2018. Time-of-addition and temperature-shift  
695 assays to determine particular step(s) in the viral life cycle that is blocked by antiviral  
696 substance(s). *Bio-Protocol* 8, e2830, 10.21769/BioProtoc.2830

697 Bordon, K.C., Wiezel, G.A., Amorim, F.G., Arantes, E.C., 2015. Arthropod venom  
698 hyaluronidases: biochemical properties and potential applications in medicine and  
699 biotechnology. *J. Venom Anim. Toxins Incl. Trop. Dis.* 21, 43, 10.1186/s40409-015-  
700 0042-7

701 Callens, N., Brugger, B., Bonnafous, P., Drobecq, H., Gerl, M.J., Krey, T., Roman-Sosa,  
702 G., Rumenapf, T., Lambert, O., Dubuisson, J., Rouille, Y., 2016. Morphology and  
703 molecular composition of purified bovine viral diarrhea virus envelope. *PLOS Pathog.*  
704 12, e1005476, 10.1371/journal.ppat.1005476

705 Carmo, A.O., Oliveira-Mendes, B.B., Horta, C.C., Magalhaes, B.F., Dantas, A.E.,  
706 Chaves, L.M., Chavez-Olortegui, C., Kalapothakis, E., 2014. Molecular and functional  
707 characterization of metallo-serrulases, new metalloproteases from the *Tityus serrulatus*  
708 venom gland. *Toxicon* 90, 45-55, 10.1016/j.toxicon.2014.07.014

709 Chang, Z., Li, G.J., Liu, J.T., Zhang, Y., Ashby, C., Liu, D.L., Cramer, C.L., Huang,  
710 X.Z., 2015. Bridger: a new framework for de novo transcriptome assembly using  
711 RNA-seq data. *Genome Biol.* 16, 30, 10.1186/s13059-015-0596-2

712 Chen, M., Aoki-Utsubo, C., Kameoka, M., Deng, L., Terada, Y., Kamitani, W., Sato, K.,  
713 Koyanagi, Y., Hijikata, M., Shindo, K., Noda, T., Kohara, M., Hotta, H., 2017. Broad-  
714 spectrum antiviral agents: secreted phospholipase A2 targets viral envelope lipid  
715 bilayers derived from the endoplasmic reticulum membrane. *Sci. Rep.* 7, 15931,

716 10.1038/s41598-017-16130-w  
717 Chen, Z.Y., Hu, Y.T., Yang, W.S., He, Y.W., Feng, J., Wang, B., Zhao, R.M., Ding, J.P.,  
718 Cao, Z.J., Li, W.X., Wu, Y.L., 2012. Hg1, novel peptide inhibitor specific for Kv1.3  
719 channels from first scorpion Kunitz-type potassium channel toxin family. *J. Biol.*  
720 *Chem.* 287, 13813-13821, 10.1074/jbc.M112.343996  
721 Chen, Z.Y., Wang, B., Hu, J., Yang, W.S., Cao, Z.J., Zhuo, R.X., Li, W.X., Wu, Y.L.,  
722 2013. SjAPI, the first functionally characterized *Ascaris*-type protease inhibitor from  
723 animal venoms. *PLOS ONE* 8, e57529, 10.1371/journal.pone.0057529  
724 Cheng, Y.T., Sun, F., Li, S., Gao, M.J., Wang, L.Y., Sarhan, M., Abdel-Rahman, M.A.,  
725 Li, W.X., Kwok, H.F., Wu, Y.L., Cao, Z.J., 2020. Inhibitory activity of a scorpion  
726 defensin BmKDfsin3 against hepatitis C virus. *Antibiotics* 9, ARTN 33,  
727 10.3390/antibiotics9010033  
728 Cid-Uribe, J.I., Meneses, E.P., Batista, C.V.F., Ortiz, E., Possani, L.D., 2019. Dissecting  
729 toxicity: The venom gland transcriptome and the venom proteome of the highly  
730 venomous scorpion *Centruroides limpidus* (Karsch, 1879). *Toxins* 11, ARTN 247,  
731 10.3390/toxins11050247  
732 da Mata, E.C., Mourao, C.B., Rangel, M., Schwartz, E.F., 2017. Antiviral activity of  
733 animal venom peptides and related compounds. *J. Venom Anim. Toxins Incl. Trop.*  
734 *Dis.* 23, 3, 10.1186/s40409-016-0089-0  
735 de Oliveira, U.C., Candido, D.M., Dorce, V.A.C., Junqueira-de-Azevedo, I.D.M., 2015.  
736 The transcriptome recipe for the venom cocktail of *Tityus bahiensis* scorpion. *Toxicon*  
737 95, 52-61, 10.1016/j.toxicon.2014.12.013  
738 Deng, L., Shoji, I., Ogawa, W., Kaneda, S., Soga, T., Jiang, D., Ide, Y.H., Hotta, H.,  
739 2011. Hepatitis C virus infection promotes hepatic gluconeogenesis through an NS5A-  
740 Mediated, FoxO1-dependent pathway. *J Virol* 85, 8556-8568, 10.1128/Jvi.00146-11  
741 Deng, Y.C., Gu, J.W., Yan, Z.P., Wang, M.D., Ma, C.Q., Zhang, J.F., Jiang, G.X., Ge,  
742 M.X., Xu, S.G., Xu, Z., Xiao, L., 2018. De novo transcriptomic analysis of the  
743 venomous glands from the scorpion *Heterometrus spinifer* revealed unique and

744 extremely high diversity of the venom peptides. *Toxicon* 143, 1-19,  
745 10.1016/j.toxicon.2017.12.051

746 Dennis, E.A., Cao, J., Hsu, Y.H., Magrioti, V., Kokotos, G., 2011. Phospholipase A2  
747 enzymes: physical structure, biological function, disease implication, chemical  
748 inhibition, and therapeutic intervention. *Chem. Rev.* 111, 6130-6185,  
749 10.1021/cr200085w

750 Dias, N.B., de Souza, B.M., Cocchi, F.K., Chalkidis, H.M., Dorcec, V.A.C., Palma,  
751 M.S., 2018. Profiling the short, linear, non-disulfide bond-containing peptidome from  
752 the venom of the scorpion *Tityus obscurus*. *J. Proteomics* 170, 70-79,  
753 10.1016/j.jprot.2017.09.006

754 Diego-Garcia, E., Peigneur, S., Clynen, E., Marien, T., Czech, L., Schoofs, L., Tytgat, J.,  
755 2012. Molecular diversity of the telson and venom components from *Pandinus*  
756 *cavimanus* (Scorpionidae Latreille 1802): Transcriptome, venomics and function.  
757 *Proteomics* 12, 313-328, 10.1002/pmic.201100409

758 El-Bitar, A.M., Sarhan, M.M., Aoki, C., Takahara, Y., Komoto, M., Deng, L., Moustafa,  
759 M.A., Hotta, H., 2015. Virocidal activity of Egyptian scorpion venoms against  
760 hepatitis C virus. *Virol. J.* 12, 47, 10.1186/s12985-015-0276-6

761 Fu, Y., Li, C., Dong, S., Wu, Y., Zhangsun, D., Luo, S., 2018. Discovery methodology  
762 of novel conotoxins from *Conus* species. *Mar. Drugs* 16, 417, 10.3390/md16110417

763 Gao, B., Dalziel, J., Tanzi, S., Zhu, S.Y., 2018. Meucin-49, a multifunctional scorpion  
764 venom peptide with bactericidal synergy with neurotoxins. *Amino Acids* 50, 1025-  
765 1043, 10.1007/s00726-018-2580-0

766 Gao, R., Zhang, Y., Gopalakrishnakone, P., 2008. Purification and N-terminal sequence  
767 of a serine proteinase-like protein (BMK-CBP) from the venom of the Chinese  
768 scorpion (*Buthus martensii* Karsch). *Toxicon* 52, 348-353,  
769 10.1016/j.toxicon.2008.06.003

770 Ghosh, A., Roy, R., Nandi, M., Mukhopadhyay, A., 2019. Scorpion venom-toxins that  
771 aid in drug development: A review. *Int. J. Pept. Res. Ther.* 25, 27-37, 10.1007/s10989-

772 018-9721-x

773 Gordon, D., Karbat, I., Ilan, N., Cohen, L., Kahn, R., Gilles, N., Dong, K., Stuhmer, W.,  
774 Tytgat, J., Gurevitz, M., 2007. The differential preference of scorpion alpha-toxins for  
775 insect or mammalian sodium channels: implications for improved insect control.  
776 *Toxicon* 49, 452-472, 10.1016/j.toxicon.2006.11.016

777 Haas, B.J., Papanicolaou, A., Yassour, M., Grabherr, M., Blood, P.D., Bowden, J.,  
778 Couger, M.B., Eccles, D., Li, B., Lieber, M., MacManes, M.D., Ott, M., Orvis, J.,  
779 Pochet, N., Strozzi, F., Weeks, N., Westerman, R., William, T., Dewey, C.N.,  
780 Henschel, R., Leduc, R.D., Friedman, N., Regev, A., 2013. De novo transcript  
781 sequence reconstruction from RNA-seq using the Trinity platform for reference  
782 generation and analysis. *Nat. Protoc.* 8, 1494-1512, 10.1038/nprot.2013.084

783 Han, F., Lu, A., Yuan, Y., Huang, W., Beerntsen, B.T., Huang, J., Ling, E., 2017.  
784 Characterization of an entomopathogenic fungi target integument protein, *Bombyx*  
785 *mori* single domain von Willebrand factor type C, in the silkworm, *Bombyx mori*.  
786 *Insect Mol. Biol.* 26, 308-316, 10.1111/imb.12293

787 Harrison, P.L., Abdel-Rahman, M.A., Miller, K., Strong, P.N., 2014. Antimicrobial  
788 peptides from scorpion venoms. *Toxicon* 88, 115-137, 10.1016/j.toxicon.2014.06.006

789 Hassani, O., Loew, D., Van Dorsselaer, A., Papandreou, M.J., Sorokine, O., Rochat, H.,  
790 Sampieri, F., Mansuelle, P., 1999. Aah VI, a novel, N-glycosylated anti-insect toxin  
791 from *Androctonus australis* hector scorpion venom: isolation, characterisation, and  
792 glycan structure determination. *FEBS Lett.* 443, 175-180, 10.1016/S0014-  
793 5793(98)01710-4

794 Herzig, V., Cristofori-Armstrong, B., Israel, M.R., Nixon, S.A., Vetter, I., King, G.F.,  
795 2020. Animal toxins - Nature's evolutionary-refined toolkit for basic research and drug  
796 discovery. *Biochem. Pharmacol.* 181, ARTN 114096, 10.1016/j.bcp.2020.114096

797 Holly, M.K., Diaz, K., Smith, J.G., 2017. Defensins in viral infection and pathogenesis.  
798 *Annu. Rev. Virol.* 4, 369-391, 10.1146/annurev-virology-101416-041734

799 Horita, S., Matsushita, N., Kawachi, T., Ayabe, R., Miyashita, M., Miyakawa, T.,

800 Nakagawa, Y., Nagata, K., Miyagawa, H., Tanokura, M., 2011. Solution structure of a  
801 short-chain insecticidal toxin LaIT1 from the venom of scorpion *Liocheles*  
802 *australasiae*. Biochem. Biophys. Res. Commun. 411, 738-744,  
803 10.1016/j.bbrc.2011.07.016

804 Housley, D.M., Housley, G.D., Liddell, M.J., Jennings, E.A., 2017. Scorpion toxin  
805 peptide action at the ion channel subunit level. Neuropharmacology 127, 46-78,  
806 10.1016/j.neuropharm.2016.10.004

807 Jimenez-Vargas, J.M., Possani, L.D., Luna-Ramirez, K., 2017. Arthropod toxins acting  
808 on neuronal potassium channels. Neuropharmacology 127, 139-160,  
809 10.1016/j.neuropharm.2017.09.025

810 Jridi, I., Catacchio, I., Majdoub, H., Shahbazeddah, D., El Ayeb, M., Frassanito, M.A.,  
811 Ribatti, D., Vacca, A., Borchani, L., 2015. Hemilipin, a novel *Hemiscorpius lepturus*  
812 venom heterodimeric phospholipase A2, which inhibits angiogenesis in vitro and in  
813 vivo. Toxicon 105, 34-44, 10.1016/j.toxicon.2015.08.022

814 Juichi, H., Miyashita, M., Nakagawa, Y., Miyagawa, H., 2019. Isolation and  
815 characterization of the insecticidal, two-domain toxin LaIT3 from the *Liocheles*  
816 *australasiae* scorpion venom. Biosci. Biotechnol. Biochem. 83, 2183-2189,  
817 10.1080/09168451.2019.1654849

818 Katoh, K., Rozewicki, J., Yamada, K.D., 2019. MAFFT online service: multiple  
819 sequence alignment, interactive sequence choice and visualization. Brief. Bioinform.  
820 20, 1160-1166, 10.1093/bib/bbx108

821 Kazemi-Lomedasht, F., Khalaj, V., Bagheri, K.P., Behdani, M., Shahbazzadeh, D., 2017.  
822 The first report on transcriptome analysis of the venom gland of Iranian scorpion,  
823 *Hemiscorpius lepturus*. Toxicon 125, 123-130, 10.1016/j.toxicon.2016.11.261

824 Krayem, N., Gargouri, Y., 2020. Scorpion venom phospholipases A2: A minireview.  
825 Toxicon 184, 48-54, 10.1016/j.toxicon.2020.05.020

826 Kubelka, V., Altmann, F., Staudacher, E., Tretter, V., Marz, L., Hard, K., Kamerling, J.P.,  
827 Vliegthart, J.F.G., 1993. Primary structures of the N-linked carbohydrate chains

828 from honeybee venom phospholipase A2. Eur. J. Biochem. 213, 1193-1204,  
829 10.1111/j.1432-1033.1993.tb17870.x

830 Lassmann, T., Hayashizaki, Y., Daub, C.O., 2009. TagDust-a program to eliminate  
831 artifacts from next generation sequencing data. Bioinformatics 25, 2839-2840,  
832 10.1093/bioinformatics/btp527

833 Lombardo, D., Dennis, E.A., 1985. Cobra venom phospholipase A2 inhibition by  
834 manoalide. A novel type of phospholipase inhibitor. J. Biol. Chem. 260, 7234-7240,

835 Luna-Ramirez, K., Jimenez-Vargas, J.M., Lourival, D.P., 2016. Scorpine-like peptides.  
836 Single Cell Biol. 5, 138, 10.4172/2168-9431.1000138

837 Luna-Ramirez, K., Quintero-Hernandez, V., Juarez-Gonzalez, V.R., Possani, L.D., 2015.  
838 Whole transcriptome of the venom gland from *Urodacus yaschenkoi* scorpion. PLOS  
839 ONE 10, e0127883, 10.1371/journal.pone.0127883

840 Luna-Ramirez, K., Quintero-Hernandez, V., Vargas-Jaimes, L., Batista, C.V.F., Winkel,  
841 K.D., Possani, L.D., 2013. Characterization of the venom from the Australian scorpion  
842 *Urodacus yaschenkoi*: Molecular mass analysis of components, cDNA sequences and  
843 peptides with antimicrobial activity. Toxicon 63, 44-54,  
844 10.1016/J.Toxicon.2012.11.017

845 Madeira, F., Park, Y.M., Lee, J., Buso, N., Gur, T., Madhusoodanan, N., Basutkar, P.,  
846 Tivey, A.R.N., Potter, S.C., Finn, R.D., Lopez, R., 2019. The EMBL-EBI search and  
847 sequence analysis tools APIs in 2019. Nucleic Acids Res. 47, W636-W641,  
848 10.1093/nar/gkz268

849 Marshall, R.D., 1972. Glycoproteins. Annu. Rev. Biochem. 41, 673-702,  
850 10.1146/annurev.bi.41.070172.003325

851 Matsushita, N., Miyashita, M., Ichiki, Y., Ogura, T., Sakuradani, E., Nakagawa, Y.,  
852 Shimizu, S., Miyagawa, H., 2009. Purification and cDNA cloning of LaIT2, a novel  
853 insecticidal toxin from venom of the scorpion *Liocheles australasiae*. Biosci.  
854 Biotechnol. Biochem. 73, 2769-2772, 10.1271/bbb.90509

855 Matsushita, N., Miyashita, M., Sakai, A., Nakagawa, Y., Miyagawa, H., 2007.

856 Purification and characterization of a novel short-chain insecticidal toxin with two  
857 disulfide bridges from the venom of the scorpion *Liocheles australasiae*. *Toxicon* 50,  
858 861-867, 10.1016/j.toxicon.2007.06.014

859 Meng, L.X., Xie, Z.L., Zhang, Q., Li, Y., Yang, F., Chen, Z.Y., Li, W.X., Cao, Z.J., Wu,  
860 Y.L., 2016. Scorpion potassium channel-blocking defensin highlights a functional link  
861 with neurotoxin. *J. Biol. Chem.* 291, 7097-7106, 10.1074/jbc.M115.680611

862 Mishra, M., 2020. Evolutionary aspects of the structural convergence and functional  
863 diversification of Kunitz-domain inhibitors. *J. Mol. Evol.*, 537-548, 10.1007/s00239-  
864 020-09959-9

865 Miyashita, M., Kitanaka, A., Yakio, M., Yamazaki, Y., Nakagawa, Y., Miyagawa, H.,  
866 2017. Complete de novo sequencing of antimicrobial peptides in the venom of the  
867 scorpion *Isometrus maculatus*. *Toxicon* 139, 1-12, 10.1016/j.toxicon.2017.09.010

868 Miyashita, M., Otsuki, J., Hanai, Y., Nakagawa, Y., Miyagawa, H., 2007.  
869 Characterization of peptide components in the venom of the scorpion *Liocheles*  
870 *australasiae* (Hemiscorpiidae). *Toxicon* 50, 428-437, 10.1016/j.toxicon.2007.04.012

871 Miyashita, M., Sakai, A., Matsushita, N., Hanai, Y., Nakagawa, Y., Miyagawa, H., 2010.  
872 A novel amphipathic linear peptide with both insect toxicity and antimicrobial activity  
873 from the venom of the scorpion *Isometrus maculatus*. *Biosci. Biotechnol. Biochem.*  
874 74, 364-369, 10.1271/bbb.90723

875 Oldrati, V., Arrell, M., Violette, A., Perret, F., Sprungli, X., Wolfender, J.L., Stocklin, R.,  
876 2016. Advances in venomics. *Mol. Biosyst.* 12, 3530-3543, 10.1039/c6mb00516k

877 Plummer, T.H., Tarentino, A.L., 1981. Facile cleavage of complex oligosaccharides  
878 from glycopeptides by almond emulsin peptide - N-glycosidase. *J. Biol. Chem.* 256,  
879 243-246,

880 Quintero-Hernandez, V., Jimenez-Vargas, J.M., Gurrola, G.B., Valdivia, H.H., Possani,  
881 L.D., 2013. Scorpion venom components that affect ion-channels function. *Toxicon*  
882 76, 328-342, 10.1016/J.Toxicon.2013.07.012

883 Quintero-Hernandez, V., Ortiz, E., Rendon-Anaya, M., Schwartz, E.F., Becerril, B.,



884 Corzo, G., Possani, L.D., 2011. Scorpion and spider venom peptides: gene cloning and  
885 peptide expression. *Toxicon* 58, 644-663, 10.1016/j.toxicon.2011.09.015

886 Quintero-Hernandez, V., Ramirez-Carretero, S., Romero-Gutierrez, M.T., Valdez-  
887 Velazquez, L.L., Becerril, B., Possani, L.D., Ortiz, E., 2015. Transcriptome analysis of  
888 scorpion species belonging to the *Vaejovis* genus. *PLOS One* 10, e0117188,  
889 10.1371/journal.pone.0117188

890 Ranasinghe, S., McManus, D.P., 2013. Structure and function of invertebrate Kunitz  
891 serine protease inhibitors. *Dev. Comp. Immunol.* 39, 219-227,  
892 10.1016/j.dci.2012.10.005

893 Romero-Gutierrez, M.T., Santibanez-Lopez, C.E., Jimenez-Vargas, J.M., Batista, C.V.F.,  
894 Ortiz, E., Possani, L.D., 2018. Transcriptomic and proteomic analyses reveal the  
895 diversity of venom components from the vaejovid scorpion *Serradigitus gertschi*.  
896 *Toxins* 10, 359, 10.3390/toxins10090359

897 Santibanez-Lopez, C.E., Cid-Uribe, J.I., Batista, C.V., Ortiz, E., Possani, L.D., 2016.  
898 Venom gland transcriptomic and proteomic analyses of the enigmatic scorpion  
899 *Superstitionia donensis* (Scorpiones: Superstitioniidae), with insights on the evolution  
900 of its venom components. *Toxins* 8, 367, 10.3390/toxins8120367

901 Schwartz, E.F., Diego-Garcia, E., Rodriguez de la Vega, R.C., Possani, L.D., 2007.  
902 Transcriptome analysis of the venom gland of the Mexican scorpion *Hadrurus*  
903 *gertschi* (Arachnida: Scorpiones). *BMC Genomics* 8, 119, 10.1186/1471-2164-8-119

904 Schwartz, E.F., Mourao, C.B., Moreira, K.G., Camargos, T.S., Mortari, M.R., 2012.  
905 Arthropod venoms: a vast arsenal of insecticidal neuropeptides. *Biopolymers* 98, 385-  
906 405, 10.1002/bip.22100

907 Sheldon, T.J., Miguel-Aliaga, I., Gould, A.P., Taylor, W.R., Conklin, D., 2007. A novel  
908 family of single VWC-domain proteins in invertebrates. *FEBS Lett* 581, 5268-5274,  
909 10.1016/J.Febslet.2007.10.016

910 Silva, E.C.N., Camargos, T.S., Maranhao, A.Q., Silva-Pereira, I., Silva, L.P., Possani,  
911 L.D., Schwartz, E.F., 2009. Cloning and characterization of cDNA sequences encoding

912 for new venom peptides of the Brazilian scorpion *Opisthacanthus cayaporum*.  
913 *Toxicon* 54, 252-261, 10.1016/J.Toxicon.2009.04.010

914 Smith, J.J., Alewood, P.F., 2015. Modern venom profiling: Mining into scorpion venom  
915 biodiversity, in: Gopalakrishnakone, P., Possani, L.D., Schwartz, E.F., Rodríguez de la  
916 Vega, R.C., (Eds), *Scorpion Venoms*. Springer, Dordrecht.

917 Smith, J.J., Herzig, V., King, G.F., Alewood, P.F., 2013. The insecticidal potential of  
918 venom peptides. *Cell. Mol. Life Sci.* 70, 3665-3693, 10.1007/s00018-013-1315-3

919 Smith, J.J., Hill, J.M., Little, M.J., Nicholson, G.M., King, G.F., Alewood, P.F., 2011.  
920 Unique scorpion toxin with a putative ancestral fold provides insight into evolution of  
921 the inhibitor cystine knot motif. *P. Natl. Acad. Sci. USA* 108, 10478-10483,  
922 10.1073/pnas.1103501108

923 Song, J., Fujii, M., Wang, F., Itoh, M., Hotta, H., 1999. The NS5A protein of hepatitis C  
924 virus partially inhibits the antiviral activity of interferon. *J Gen Virol* 80, 879-886,  
925 10.1099/0022-1317-80-4-879

926 Soudani, N., Gharbi-Chihi, J., Srairi-Abid, N., Martin-El Yazidi, C., Planells, R.,  
927 Margotat, A., Torresani, J., El Ayeb, M., 2005. Isolation and molecular  
928 characterization of LVP1 lipolysis activating peptide from scorpion *Buthus occitanus*  
929 *tunetanus*. *BBA-Proteins Proteom.* 1747, 47-56, 10.1016/j.bbapap.2004.09.020

930 Staudacher, E., Altmann, F., Marz, L., Hard, K., Kamerling, J.P., Vliegenthart, J.F.G.,  
931 1992. Alpha-1-6(alpha-1-3)-difucosylation of the asparagine-bound N-  
932 acetylglucosamine in honeybee venom phospholipase-A2. *Glycoconjugate J.* 9, 82-85,  
933 10.1007/Bf00731703

934 Teixeira, S.C., Borges, B.C., Oliveira, V.Q., Carregosa, L.S., Bastos, L.A., Santos, I.A.,  
935 Jardim, A.C.G., Melo, F.F., Freitas, L.M., Rodrigues, V.M., Lopes, D.S., 2020. Insights  
936 into the antiviral activity of phospholipases A2 (PLA2s) from snake venoms. *Int. J.*  
937 *Biol. Macromol.* 164, 616-625, 10.1016/j.ijbiomac.2020.07.178

938 Valdez-Cruz, N.A., Batista, C.V.F., Possani, L.D., 2004. Phaiodactylipin, a glycosylated  
939 heterodimeric phospholipase A2 from the venom of the scorpion *Anuroctonus*

940 *phaiodactylus*. Eur. J. Biochem. 271, 1453-1464, 10.1111/j.1432-1033.2004.04047.x  
941 Vetter, I., Davis, J.L., Rash, L.D., Anangi, R., Mobli, M., Alewood, P.F., Lewis, R.J.,  
942 King, G.F., 2011. Venomics: a new paradigm for natural products-based drug  
943 discovery. Amino Acids 40, 15-28, 10.1007/s00726-010-0516-4  
944 Walker, A.A., Robinson, S.D., Hamilton, B.F., Undheim, E.A.B., King, G.F., 2020.  
945 Deadly proteomes: A practical guide to proteotranscriptomics of animal venoms.  
946 Proteomics 20, ARTN 1900324, 10.1002/pmic.201900324  
947 Walski, T., De Schutter, K., Van Damme, E.J.M., Smagghe, G., 2017. Diversity and  
948 functions of protein glycosylation in insects. Insect Biochem. Mol. Biol. 83, 21-34,  
949 10.1016/j.ibmb.2017.02.005  
950 Wang, H.D., Smagghe, G., Meeus, I., 2017. The role of a single gene encoding the  
951 single von Willebrand factor C-domain protein (SVC) in bumblebee immunity extends  
952 beyond antiviral defense. Insect. Biochem. Mol. Biol. 91, 10-20,  
953 10.1016/j.ibmb.2017.10.002  
954 Ward, M.J., Ellsworth, S.A., Rokyta, D.R., 2018. Venom-gland transcriptomics and  
955 venom proteomics of the Hentz striped scorpion (*Centruroides hentzi*; Buthidae)  
956 reveal high toxin diversity in a harmless member of a lethal family. Toxicon 142, 14-  
957 29, 10.1016/j.toxicon.2017.12.042  
958 Wullschleger, B., Nentwig, W., Kuhn-Nentwig, L., 2005. Spider venom: enhancement  
959 of venom efficacy mediated by different synergistic strategies in *Cupiennius salei*. J  
960 Exp Biol 208, 2115-2121, 10.1242/jeb.01594  
961 Yacoub, T., Rima, M., Karam, M., Fajloun, J., 2020. Antimicrobials from venomous  
962 animals: An overview. Molecules 25, 2402, 10.3390/molecules25102402  
963 Yang, Y., Zeng, X.C., Zhang, L., Nie, Y., Shi, W.X., Liu, Y.C., 2014. Androcin, a novel  
964 type of cysteine-rich venom peptide from *Androctonus bicolor*, Induces akinesia and  
965 anxiety-like symptoms in mice. IUBMB Life 66, 277-285, 10.1002/iub.1261  
966 Yi, H.Y., Chowdhury, M., Huang, Y.D., Yu, X.Q., 2014. Insect antimicrobial peptides  
967 and their applications. Appl. Microbiol. Biot. 98, 5807-5822, 10.1007/s00253-014-

968 5792-6

969 Zeng, X.C., Nie, Y., Luo, X.S., Wu, S.F., Shi, W.X., Zhang, L., Liu, Y.C., Cao, H.J.,  
970 Yang, Y., Zhou, J.P., 2013. Molecular and bioinformatical characterization of a novel  
971 superfamily of cysteine-rich peptides from arthropods. *Peptides* 41, 45-58,  
972 10.1016/j.peptides.2012.10.004

973 Zhang, L., Shi, W.X., Zeng, X.C., Ge, F., Yang, M.K., Nie, Y., Bao, A., Wu, S.F., E,  
974 G.J., 2015. Unique diversity of the venom peptides from the scorpion *Androctonus*  
975 *bicolor* revealed by transcriptomic and proteomic analysis. *J. Proteomics* 128, 231-  
976 250, 10.1016/j.jprot.2015.07.030

977 Zhao, R.M., Ma, Y.B., He, Y.W., Di, Z.Y., Wu, Y.L., Cao, Z.J., Li, W.X., 2010.  
978 Comparative venom gland transcriptome analysis of the scorpion *Lychas mucronatus*  
979 reveals intraspecific toxic gene diversity and new venomous components. *BMC*  
980 *Genomics* 11, 452, 10.1186/1471-2164-11-452

981 Zhao, Y., Chen, Z., Cao, Z., Li, W., Wu, Y., 2019. Diverse structural features of  
982 potassium channels characterized by scorpion toxins as molecular probes. *Molecules*  
983 24, 2045, 10.3390/molecules24112045

984 Zhong, J., Zeng, X.C., Zeng, X., Nie, Y., Zhang, L., Wu, S., Bao, A., 2017.  
985 Transcriptomic analysis of the venom glands from the scorpion *Hadogenes troglodytes*  
986 revealed unique and extremely high diversity of the venom peptides. *J. Proteomics*  
987 150, 40-62, 10.1016/j.jprot.2016.08.004

988 Zhu, S., Gao, B., 2006. Molecular characterization of a new scorpion venom lipolysis  
989 activating peptide: Evidence for disulfide bridge-mediated functional switch of  
990 peptides. *FEBS Lett.* 580, 6825-6836, 10.1016/j.febslet.2006.11.040

991 Zhu, S.Y., Peigneur, S., Gao, B., Umetsu, Y., Ohki, S., Tytgat, J., 2014. Experimental  
992 conversion of a defensin into a neurotoxin: Implications for origin of toxic function.  
993 *Mol. Biol. Evol.* 31, 546-559, 10.1093/molbev/msu038

994

Table 1 List of the peptide fragments generated by enzymatic digestions

| Peptide sequence                                | Molecular mass (Da) |         | Mass difference |
|---|---------------------|---------|-----------------|
|   | Obs.                | Calc.   |                 |
| <i>Lys-C digestion</i>                          |                     |         |                 |
| LIFPGTK   | 774.46              | 774.47  | -0.01           |
| WCGAGDK   | 793.30              | 793.31  | -0.01           |
| AANYSDLGSA AETDK                                | 2209.90             | 1511.68 | 698.22          |
| CCRAHDHCDNIAAGETK                               | 2016.74             | 2016.78 | -0.04           |
| YGLENSYWFTK                                     | 1406.63             | 1406.66 | -0.03           |
| CEESFRNCLAEAK                                   | 1614.64             | 1614.67 | -0.03           |
| FSYFNVYGP K                                     | 1220.57             | 1220.59 | -0.02           |
| CFVLDCD   | 929.30              | 929.32  | -0.02           |
| <i>Lys-C digestion after PNGase A treatment</i> |                     |         |                 |
| AADYSDLGSA AETDK                                | 1512.69             | 1512.67 | 0.02            |
| <i>Glu-C digestion</i>                          |                     |         |                 |
| LIFPGTKWCGAGDKAANYSDLGSA AE                     | 3397.39             | 2699.25 | 698.14          |
| TDKCCRAHDHCDNIAAGETKYGLE                        | 2823.04             | 2823.16 | -0.12           |
| NSYWFTKLNCKCEE                                  | 1879.70             | 1879.78 | -0.08           |
| SFRNCLAE  | 996.40              | 996.44  | -0.04           |
| TTAKFVKFSYFNVYGP KCFVLDCD                       | 2907.22             | 2907.36 | -0.14           |

Table 2 Virucidal activity of LaPLA<sub>2</sub>-1

| Virus             | IC <sub>50</sub> (ng/ml) <sup>a</sup> |
|-------------------|---------------------------------------|
| HCV               | 2.0 ± 0.3                             |
| HCV (+ manoolide) | >500                                  |
| DENV              | 3.4 ± 0.6                             |
| JEV               | 5.7 ± 0.8                             |
| HSV-1             | >1,000                                |

<sup>a</sup> The data represent means ± SEM from three independent experiments.

Table S1 Sequences of peptides identified by the transcriptome analysis of the venom gland.

| Name  | Sequence  | Similar peptide (Accession number, species)         |
|---|---|---|
| <b>Non-disulfide-bridged peptide</b>                |   |   |
| LaNDBP2-1   | MNIKVVLVCLITLLVTEQVEGGWFSRIKSLAKKAWKSNLAKDLRKMAGKAARNYA AKVLNVSPEEQVQLDNLLRYLD    | Vejovine (F1AWB0, <i>Vaejovis mexicanus</i> )       |
| LaNDBP2-2   | MNGKVLVCLIVAMLVMEPAEAGIWGWIKKTAKKVWNSDIANQLKNKALNAAKNYVAEKVGATPAEAGQMPFDEFMDIYYS  | Con22 (L0GBQ6, <i>Urodacus yaschenkoi</i> )         |
| LaNDBP3-1   | MQYKTFVLVIFLAYLLVTEEAQAFWWALAKGAAKLLPSVVGAFTRKREIEKIFDPYQSSLDLEMERFLRQLQ          | Heterin 2 (AGK88595, <i>Heterometrus spinifer</i> ) |
| LaNDBP3-2   | MKLRTLMVIFLAYLIVTDEAEAFWGF LAKAAKLLPSLFSSKKEKEKREIEHFFDPYEKELDSELDQLLYELQ         | Heterin 2 (AGK88595, <i>Heterometrus spinifer</i> ) |
| LaNDBP4-1   | MKIQLAILVITVVLQMQLVQTEAGFWGKLWEGVKNVIGKRGLRNKDQLDDLFDSDLSADAKLLREMFK              | OcyC2 (C5J887, <i>Opisthacanthus cayaporum</i> )    |
| LaNDBP4-2   | MKIQLAILVITVVLQMQLVQTEASFWGKLWEGVKS AIGKRGLRDVDQMDDLFDSDLSADAKLLREIFK             | OcyC2 (C5J887, <i>Opisthacanthus cayaporum</i> )    |
| LaNDBP4-3   | MKNQFVILLIAVFLQLFSQSEAFLSALWGVAKSLFGKRGLK NLDQLDDLFDGEVSEADLDFLKELMR              | UyCT3 (L0GCI6, <i>Urodacus yaschenkoi</i> )         |
| LaNDBP4-4   | MKAQIVLLVITVVLQMFAQSEAGFWGKLWEGVKS AIGKRGLRNLDQFDELFDSDLSADAKLLKEIFK              | UyCT1 (L0GCV8, <i>Urodacus yaschenkoi</i> )         |
| LaNDBP4-5   | MRLVSLTPLFLILLIAVDYQCQSFPLL SLIPSAISALKKLGKRSTDFQRQLDFQRRYLNSDLDFDLDELEEF LDQLPDY | VpAmp1.0 (ALG64974, <i>Vaejovis punctatus</i> )     |
| <b>Invertebrate defensin</b>                        |   |   |
| LaDefensin1   | MKAIATLLLLLVAFSVLEFGIVDAGFGCPFNRYQCHSHCQS IRRGGFCAGTFRTTCTCYKSK                   | AbDef-1 (AIX87626, <i>Androctonus bicolor</i> )     |
| LaDefensin2   | MKAIATLLLLLVAFSILEDGIVDAGFGCPFNRYQCHSHCRS IRRGGYCSGPFRTTCTCYK                     | AbDef-1 (AIX87626, <i>Androctonus bicolor</i> )     |
| LaDefensin3   | MKAIATLLLLLA FSI LEFGIVGAGFGCPHNRYQCHSHCQS IGRNGGYCGGTFRTTCTCYNSGGPTSSP           | AbDef-1 (AIX87626, <i>Androctonus bicolor</i> )     |
| <b>Potassium channel toxin-like peptide (alpha)</b> |   |   |
| La-alphaKTx1  | MNAKFIYILLTAVMFALYEASVPPNIPCQVTNQC PKPCREATGRPN SKCINGRCKCYG                      | Urotoxin (P0DL37, <i>Urodacus yaschenkoi</i> )      |
| La-alphaKTx2  | MNTKFVLLLLVISTLMPTFDASAEDISCS SSKECYDPCEEETGCSSAKCVGGWCKCYGCRG                    | Urotoxin (P0DL37, <i>Urodacus yaschenkoi</i> )      |
| La-alphaKTx3  | MNRNFVLLLLLIVTLMPMLDAATEDINCDNWRDCLKPCK DETGCPNSKCEE GNCLCYGCNRLTV                | Urotoxin (P0DL37, <i>Urodacus yaschenkoi</i> )      |
| La-alphaKTx4  | MNKKFIFLLLVTTLMPMFDAATEAISCSNPND CREPCKKQTGCSGGKCMNRKCKCHRCNG                     | OckTx2 (Q6XLL8 <i>Opisthophthalmus carinatus</i> )  |
| La-alphaKTx5  | MNAKLV CIVLLTAVMFAPDEASLPPIRIPCYSKDCRKPCLYLTGTPRSKCINRRCKCYG                      | Hemitoxin (P85528, <i>Hemiscorpius lepturus</i> )   |
| La-alphaKTx6  | MNKPFCAIFLVLMFAVSVLPAESTGGCPVDSLCKSYCKSNKFGTEGKCDGT SCKCAIG                       | LmKTx8 (A9QLM3, <i>Lychas mucronatus</i> )          |
| La-alphaKTx7  | MNKLACYILICVMVSCLFKVPVAEGISAGCPLTAKLCTIYCKK HRFREGK CIGPTRFRCKCYV                 | LmKTx8 (A9QLM3, <i>Lychas mucronatus</i> )          |

|   |  |  |
|---|--|--|
| La-alphaKTx8  | MRLVILLMLTTLVLA VGAPLGGAKCSSSTQCTRPCRYAGGTHGKCMNGRCRCYG  | St20 (P0DP36, <i>Scorpiops tibetanus</i> )               |
| La-alphaKTx9  | MELKYLLVLLAVTCLVSCQDNSLLPSGSCSRTGICMESCAPFLYQPKYHRRCPAGYVCCTLIY  | Kbot55 (P0DL62, <i>Buthus occitanus tunetanus</i> )      |
| <b>Potassium channel toxin-like peptide (beta)</b>  |  |  |
| La-betaKTx1 (LaIT2)                                 | MAKHLIVMFLVIMVISSLVDCAKKPFVQRVKNAASKAYNKLKGLAMQSQYGCPIISNMCEDHCRRKKMEGQCDDLDCVCS                             | Previously identified                                    |
| La-betaKTx2 (LaIT3)                                 | MQAQFTVLLLLVLVTLCSGGILREKYFHKAADALTSNIPIPVVKDVLKSAANQMIRKIGKVQQACAFNKDLAGWCEKSCQEAE<br>GKKGYCHGTKCKCGKPIDYRK | Previously identified                                    |
| La-betaKTx3   | MDTKLSILVFLCVVVIASCSWISEKRIQKALDEKLPKGFIQGAAKAIVHKFAKNQYGCLADMVKGSCDRHCQETESTNGVCHG<br>TKCKCGIGRVY           | SCI1 (L0G8Z0, <i>Urodacus yaschenko</i> )                |
| <b>Potassium channel toxin-like peptide (delta)</b> |  |  |
| La-deltaKTx1  | MASQFLLFCIVLIAVNPLVYSKGGCRLPPETGLCYAYFERYYYYDPSSNNCKMFVYGGCGGNSNNFVSKKACLARCAN                               | BmKTT-2 (P0DJ50, <i>Mesobuthus martensii</i> )           |
| <b>Potassium channel toxin-like peptide (kappa)</b> |  |  |
| La-kappaKTx1  | MKPSTSAYALLLVLTFGIITSGVFAVPMDEENTFEVEKRGNSCMEVCLQHEGNVAECEEKACNKG  | HeTx203 (P0DJ34, <i>Heterometrus petersii</i> )          |
| La-kappaKTx2  | MKPSTSAFILLLVLTFGIITSGVSAIPMDEENTFEEQKRDSACVEVCLHHEGNVAECEEACKKS   | HeTx203 (P0DJ34, <i>Heterometrus petersii</i> )          |
| La-kappaKTx3  | MKLLPLLVIILICALMANEAFCDQGARERSENLEDTRDLVQKPCRIVCSENMRKICRRCTLGR  | HelaTx1 (P0DJ41, <i>Heterometrus laoticus</i> )          |
| La-kappaKTx4  | MKPSSFALIALLVFLGFTNAVSGEYAESISGDRMERAERAGCRIRCLQFTDDFEKCRKLCG  | PcavC10 (AEX09227, <i>Pandinus cavimanus</i> )           |
| La-kappaKTx5  | MKLLPLLLVILVCALLPNEAFCDQSAVERSESLEEVSREIVKRSCKRVCSTRRTRKCMQKCKSQPGR  | HelaTx1 (P0DJ41, <i>Heterometrus laoticus</i> )          |
| <b>DDH peptide</b>                                  |  |  |
| LaDDH1 (LaIT1)                                      | MNFATKVFFLLLAVAVIAIVAGEEDDSWFEEQNEESDTERDFPLSKEYETCVRPRKCQPPLKCNKAQICVDPKKGW                                 | Previously identified                                    |
| LaDDH2  | MNCAIKVSFLLLAITVIFSVAGGEGDNSFEQREENDTERDLPLSKKHESCVRPRKCRPPLRCNAHICVESKKGWRIPVISWVS<br>KTKIMFSE              | LaIT1 (P0C5F2, <i>Liocheles australasiae</i> )           |
| <b>Sodium channel toxin-like peptide</b>            |  |  |
| LaLAP1  | MNTGEHFASLIIFLLLLGENPCLGDGGWPMRIDGNYYLCYEEKPAELYCKRACKLHKASQSSCSYHWKYMSWYCYCEDLKK<br>GYTRDRGLKKGQGHQFSES     | LVP1-alpha (P0CI45, <i>Lychas mucronatus</i> )           |
| LaLAP2  | MLMVIYIATLIPLILQGECRAKDDHPRNFEGNCYRCKYDPKSGYCEAICKMHAETGYCSRSNLCYCKGIEDKYVSARDFLEP                           | BmLVP1-alpha (Q6WJF5, <i>Mesobuthus martensii</i> )      |
| <b>La1-like peptide</b>                             |  |  |
| La1   | MGGTLKHLVVCLIVCSSSLCLGFGESCIAGRIVPLGQQVTDQRDCALYKCVNYNKKFALETKRCATVNLKSGCKTVPGGA<br>GAAFPSCCPMVTCKG          | Previously identified                                    |
| La1-1   | MKHLHAAVLLVCLSICALPSLTLGAGESCKVGSVIPVGQKKFDKPSCAEYECSTEFNRVLLKAITCATLNTKKGKCKSVPGKS<br>PNSFPDCCPTILCRGEQWNH  | La1-like protein 15 (L0GB04, <i>Urodacus yaschenko</i> ) |



|       |  |  |
|-------|--|--|
| La1-2 | MKIVCTLVPLVFACIANAHVLTERTCRTHTGVLKNGEEWADPNHCSIYRCTIYSGEAELQGLTCATYRVPPNCEFVRGRGKFY<br>PSCCPTVMCKP                                       | OcyC11 (C5J895, <i>Opisthacanthus cayaporum</i> )            |
| La1-3 | MALRFVLAFLLPCLVLGSNEPAKFISYKNDMLGPLVEGKCKVGNKMIQQGGTWYRDDYCEKIYCLRTGTLGHMEVWGCAPV<br>APLNPNTVVHHSGLYPNCCSGEIVCEENPDTKKSDVEMAEIIRALLQSERK | MeVP-7 (ABR21061, <i>Mesobuthus eupeus</i> )                 |
| La1-4 | MFNIVTITLLWSCTCIALCHSYGETCQAGELTIPLDNEKQDPEACTLYKCTMFAGRVVNLTLTCAPQEPRRGCRNVDSPVELPF<br>PDCCPLVVCNVQPLGSK                                | HsVx1 (K7WMX6, <i>Heterometrus spinifer</i> )                |
| La1-5 | MRTLVPVAVFLLALIVAAMASHKDPYHRNCPIGNKDLSDGEEWADQQRVCVKYKQIRGPDAALLLTRCPVSGIYPPDKCREIAG<br>KGNFPDCCPKLQCD                                   | MmKTx1-like (XP_02321219, <i>Centruroides sculpturatus</i> ) |
| La1-6 | MSRADKAFVGTLIAIFLVCSLTNAYSSLKRQKYGSGAPCVDHLGNSNRKFDVWYDNESCEEHTCIKYRGIPHVQIYGCIAAVAS<br>PGCELVKGSGSYPDCCCEEEIC                           | TxLP9 (ABY26691, <i>Lychas mucronatus</i> )                  |
| La1-7 | MKTWEARFYIFLVALVTITFVESYVYLVLPQDPGAVVCIGKDRVSHKPGDVWYDDSKCERLTCGHSSGGLVIDGAGCGSISVQD<br>GCKLVPGVGSYPSCCPSPVC                             | Toxin-like protein 14 (L0GCW8, <i>Urodacus yaschenko</i> )   |

---

**Serine protease inhibitor-like peptide**

---

|        |   |   |
|--------|---|---|
| LaAPI1 | MKSWTYRLCFLILFLVCVNCTRPVLSPEECTRPGEFFTTAGSYCPLTCDNYKNPPIICSLIGVGCESPELVRDERSGNCVDTS<br>DCTED        | SjAPI (P0DM55, <i>Scorpiops jendeki</i> )       |
| LaAPI2 | MKGFAFLVLTFFVVFGDKEQECEDPNAEFRRCNTACPITCANMDNPPNICTLQCVIGCACKEGYKNDGGLCVHPEGC                       | SjAPI (P0DM55, <i>Scorpiops jendeki</i> )       |
| LaAPI3 | MKALLLLLSFVVIHSAKSQEDLGGDEHAQSCLLPNEVWDKCGPSCPPSCIGVIEPGTLCSTECTPGCFCREGLVRTKRGSCIPP<br>KACRNERETKL | SjAPI-2 (P0DM56, <i>Scorpiops jendeki</i> )     |
| LaAPI4 | MKGSKPLCFLYLVVLLWTSVKCTRWASSEECTRPGEAFTSCGTDCPITCANYENPPEFCNYMCVIGCECTSGLVRDEGSGN<br>CVNPSQCGP      | HtPi1 (AOF40217, <i>Hadogenes troglodytes</i> ) |
| LaAPI5 | MKRNLVLLAFVLLLFSGSIFEKCSAQRGGADRRRCPGEVFMNCGPSCPLTCDNYQNPPTVCTLQCVIGCFRRGLVRDTRRG<br>GCVRPSQCRR     | HtPi1 (AOF40217, <i>Hadogenes troglodytes</i> ) |
| LaAPI6 | MKRNLALSALFVLLFCSALDNCEAQRGGYDRTCQLEGEVFTRCGTACPLTCDNYKNPPEVCTLQCIIGCVCGRGWVKDTRRG<br>RCVRPSQCRR    | HtPi2 (AOF40218, <i>Hadogenes troglodytes</i> ) |
| LaAPI7 | MKSNLVLFVAFVLLFCSVLEICTAQRVVDRSCRGAGEVFTRCGTACPLTCDNYRNPPRFCTRQCIIGCACRRGWVKATRRG<br>GCVRPSQCRR     | HtPi2 (AOF40218, <i>Hadogenes troglodytes</i> ) |
| LaAPI8 | MAKTAFGVVLCMFVLAQSAPQYPGTFGCDEDKQFVRCLPPCPVTCKSILNTPCTLLLPRCTPGCGCRGGKILDNAGKCVFP<br>ADCRRG         | CtAPI (P0DM57, <i>Chaerilus tricostatus</i> )   |

---

Table S2 Sequences of proteins identified by the transcriptome analysis of the venom gland

| Name                               | Sequence  | Similar protein (Accession number, species)                        |
|------------------------------------|---|--|
| <b>Phospholipase A<sub>2</sub></b> |   |  |
| LaPLA <sub>2</sub> -1              | MVFIFLAVLSGLVTLSSHSTAVQREMHHVFEPLPGQRDSWPVARAALVNLATKSETGREFSDCRMNSIDEIAREGAVLSRYEIK<br>RVSKEEMRSLEKRCSSRSGIHQRLIFPGTKWCGAGDKAANYSDLGSA AETDKCCRAHDHCDNIAAGETKYGLENSYWFTKLN<br>CKCEESFRNCLAEAKKKETTAKFVKFSYFNVYGPCKFVLDCKRRFEMSRKCVAHWKESRRG  | Hemilipin (A0A1L4BJ46, <i>Hemiscorpius lepturus</i> )              |
| LaPLA <sub>2</sub> -2              | MMVSSLLIVLIVTSAVQCYYIDNMNDEEPLVTFYREKDGRRRTVEVIEVNDNKKGPKIVGCVEYGDGYIADMVNLNLSRNILVRDVN<br>RQQMDEVVNR CRERETRDLRNEVINLFKSPAETSRNAFQSLMIFPGTKWCGAGNVSENYDDLGTARATDMCCRDHDHCND<br>SIERFGSKHGLENTDFYTKSNDCDCDNKLYSCLEASKDVTSDLVG YLYFNIMQTQCFKYYPEVKCLKTKTGILFFMQSCQEYEF<br>NRNEPKKYEFFDAKYEPQAASLEQIMSYFYSSSSQ  | Phaiodactylipin (Q6PXP0, <i>Anuroctonus phaiodactylus</i> )        |
| LaPLA <sub>2</sub> -3              | MSLQTLAVLLLSFIQPLPTAVIELPHENKLTGYQNERSPYMLIIGQTGKVIHCHQYEDKNEADRVLAALKLEDVERVTKEQMDK<br>LIKFCTEEEHMGHPKEQVKMLIYPGTKWCGMGNNAASENELGTEKEADSCCREHDHCSDSIPAFSIKYNLTNYSPTKSNKNC<br>DREFRQCLTKAGTKASEIISGLYFDLLKMECFGR TSCSSNDACTEGWQWKRSTSF  | Hemilipin (A0A1L4BJ46, <i>Hemiscorpius lepturus</i> )              |
| <b>Serine protease</b>             |   |  |
| LaSP1                              | MKYASLIASVFLLTQTEACTETGEHNQIRFPEEEEEESCRTPNRRRGVCPVPLNACPEFRNADDRYIRQSIWFDNRTPVCCPS<br>NEQPVTMPHTRPTRPTRPTQPPTCPPVSPVTRCPVVGPNRRKPSILPEECGKSTVPLSRIVGGRKSDLGAWPVMVA<br>YLTRAGLNRGTDCGGSLISDKHVLTA AHCYVDKRRKTVMSASQLMVRVGEHTLNDNDGASPIDVPVSNIMAHENFERKTFK<br>NDIAILVLANTVQFSQFIRPICLPYDESSEANFTGRSAFVAGWGETEYEGQFNPELSEIQIPILNNEVCRQKYKRNIPTAEYLCA<br>GVSDGTDKDCRSDSGGPLMLPEKDNRFYLIGVVSFGKRCATYGYPGVYTRMTMYLDWLASKLS | Serine protease 1 (AMO02563, <i>Tityus serrulatus</i> )            |
| LaSP2                              | MWARFGLTFLFCYYLQNTFIGAEAQACGTRNMTLEFKIVGGTVAARGEPWQVSVQLTHPQFGKIGHWCGGLVGGQWVA<br>TAAHCIINPLFSLPQPVFVKVLLGDHIIKTEGSEVVIGVSRVYYPWYHGYQNDIALLLKSEPVKLSSYIQPICLPTSNDGFQD<br>MTCTATGWGKTDFNMKASDTLQKVDVKVLDNSICANAYLTQFKIPITPSHLCAGDTAGGKGTCLGDSGGPLQCLMPNGKWYL<br>AGLTSFGSGCAKPGFPDVYTRVYVVDWIKQNQLLPW   | Serine protease 1 (AMO02563, <i>Tityus serrulatus</i> )            |
| LaSP3                              | MNLIGLVALACVTLSSRVEARFLHDPSEESGRVFRGRFANQQEFPWMVHLQISKGNMNASVCGG SVISKNWVLTAAHCVCRN<br>ATLKYADVNGITGRIGHVNKSSATAVKFSQLIVHNSYDEDFNADIALLKFKDSLKDYANVNRICLADKGTFFPNRQPVIQMG<br>WGRFDNSSAGTSPSLKTT SVGYILHRADCIEQESYADPGQICVSNFKGEKICGGDSGGPLVANGAEKLDIGIVSYDYYSFCV<br>AGSDSPAMYTEISYYADWIKTKTNDKEICWKK  | Chymotrypsin-like protease-3 (ABR21040, <i>Mesobuthus eupeus</i> ) |
| LaSP4                              | MLWSTRDSAIFLLFIITLNSRFNYSSNQGFLLNRRSDGNTCTRNGEVHQCQFFLFCLLGGGTSMGSCSGRVLTTCCA KPNLRR<br>SRPSNFRQRALNNKDRASCQTAWKPQSRIVGGQDALYGEFPWQAHIIKIQQC GGIVSPYFVVTAAHCVYRARLHQITVVL<br>GAYDIHDQSFQLQPALFLRVDEKRLHPNFKFSHPDRYDVALLRLHRRVQYQENILPICLPPYKWNFRGWRVAVIGWGKTD<br>ALRNRYGTRLLQKVEVPIISNDECEYWHKSRGIKLIYPEMICAGYEHGKKDACVGDSSGGLMVNMRGKWTLVGITSAGFGCA<br>QWRQPGIYHSVSSTVDWINANIR  | Serine protease 3 (AMO02565, <i>Tityus serrulatus</i> )            |

|                                    |   |   |
|------------------------------------|---|---|
| LaSP5                              | MAISLLVKYAILWISLAVLSSAQSALPDRRPNFVFPETVRDSPRCRTADGSPGSCLKASECRDVNFQRGTLPLLCYWEDNQPI<br>VCCADRSAAISSENLSEPQTGCGKSERKPTTRSPTIAGGWISQPSAWPVMVAILTSNLGEKFLCGGTLVSQKYVLTAAHCFRR<br>NGVDQRRIPVARFLVRVGSTENNQGTAYRIRRIHEDYRVNQHYNDIAVIEVNDPISLSSSVRPICLPSELQGRSVVGREVVV<br>VGWGDQSFGGIRDNLREVNIVIDRDTCNEAYNELSSRSIPNGITSQFMCAGDPEGGKDACQADSGGPLMMFSPSQWSIVG<br>VVSFGYGCAHKGFPGVYTQVSSYLNWIKDKTDL   | HLClotting-factor1 (API81376, <i>Hemiscorpius lepturus</i> )                    |
| LaSP6                              | MAMKYFVLFISTNALLAASFLPAKEENRIFKGREANEGEFPWMVFIRLTDELNCSGFLVSHNYVVTAAHCMIRSVTDMKGVVGS<br>VDREQDNMLEFEKQVIHPEYNESTFHGDVALLKLRPLEFTSLIKPICIGKKSFINPGENVLQMGWGRDRNDSAVVSKILKVTN<br>VGSVMSEEHCHTFLGMINFTSIGRICVKNGEVEGVCEGDSGGPLVYKDSEHGNVAVGLSSFGFYLNCSVTNENPEIFTSTAYF<br>SNWIAENVEDSVCVIG  | Chymotrypsin-like protease-1 (ABR21038, <i>Mesobuthus eupeus</i> )              |
| LaSP7                              | MFKSFELIYLAIACIGSGSVIFAKNCDDCILITSCPGAVYLAVHAKNAKTEDLIKHSLCSLEKVNGLPKVCCSEFPAPQLDNHPN<br>LELLPKDCGEIEGSRIVGGEVAKLYEFPWMLISYDTRIGREFLCGGLISPLYVLTAAHCVHGRKIAGVRIGDYDWRKIDCEK<br>DTNLCESYYQDIGVSERLPHPDYQGGPPVVRNDIALLRLRRPVNLTVKNAGVICLPVTKELRERRLDTEQVTVAGWGITENNTAS<br>SVLLKVNLPVHSGEMCRAYYGRNSKEDTTKNILCAGVLGKDSCKGDSGGPLMLEGNYDNVFKFIQYGVSYGPSQCGSNFPG<br>VYTDVSSFMKWILDNIKP   | HLClotting-factor2 (API81377, <i>Hemiscorpius lepturus</i> )                    |
| LaSP8                              | MKCF AFLIFSSQLFPAVPFQVEEKTRIFGGREANDGEFPWMVFIRLSAEWNCGGFLISPSYVLTAAHCVKGSVTDMRGVVGS<br>VDREQDMLFEFKYQIHPEYGPKRWRNADLALLELRTPLGFTDLIKPICIGKKSFTTRPGNAVLQMGWGRDRREDSAVVTKKLK<br>VTEVGNLMSRCDCHRFESINIVDIQLNGRLCVKNREVEGVCEGDAGSPLVYQYAESSHVAIGVSAAGFYVNCSTNENPEIYT<br>DLAYYSDWIIRTVDIPII  | chymotrypsin-like protease-1 (ABR21038, <i>Mesobuthus eupeus</i> )              |
| <b>Alpha-amylase</b>               |   |   |
| La-alpha-<br>amylase               | MIVDCLLLWFVWSVHCSYHEPNTQAGRSVLVHLFEWRWKDIAEECETFLGPYGFGGVQVSPANENGIWEPHWNSVIRRP<br>WFERYQPVSYKIATRSGNESEFRDMVRRCCNAGVRIYVDAVINHMTGDIGRKGKTGGSDFDPGALQYYGVYPYGPSDFNGRD<br>QCPSGSGDIENYQDKYQVRNCRSLGLADLNLKEYVRDKIVEYLNFLIDIGVAGFRVDASKHMPGDLKIIYEKLNLTNEYFP<br>VHRRPFIYQEVIDLGGGEAVKAEYTDLGRVTEFRFGKHLGDVIRKYNQRLKYLKNFGQDWGMVSGSNALTFIDNHDNQRG<br>HGAGGFGSILTFEESRMKMAVAFMLAWPYGLPRVMSSYNWPRYVENGGKDKNDWIGPPHDDEYNTKPVVRNPDLTCGNGW<br>VCEHRWHQIYSMVKFHNVAGFEPVDFWWDNDYQQIAFGRKGKGF LAINNENHNLDQTLPTGLPPGTCDVISGKLEGDKCT<br>GRSVKVEQDGKAKIFIDNSWEDPMLAIHVEAKLNDVLHNGNTGRNRNG | Pancreatic alpha-amylase-like (XP_023225708, <i>Centruroides sculpturatus</i> ) |
| <b>Cysteine-rich venom protein</b> |   |   |
| LaCRVP1                            | MMHFILTCILFPQVIHLNGVVAKEIKYIFYSESDYCVLGERDCNTSIYAEDFLWPHNSNRAYMASGDVPELSASNMLKLEWDQN<br>LANIAQRAAEQCIDDYPTFHGKVECRQPDSSAVINFSWKQSQNLNENAKRIEERIFEWTEYIKYRYNDSSLHFYRGTGIFEDL<br>WAKVVQATTWKVGCGLADSDAVNHDMEHYTEVISCLYENTKLQPGDEIYKLGSPCSACPLGTRCIPGSNLCEVEPGNCP<br>GNAKQDCAKNTERTNRETLWKCDLKKGEECEIVPSCSLLWSVDQQGNFKSISVTRDCV SANVFIKRIRIGKPSCTTFQYIKE<br>GNRNEPSDVTVMGMVFNLES GDIIQVAKGEDATTWTDVMIDIPWTGVDIQVGVARSFNDNFRKQILMKDFHVS DSA CLR D<br>TEHFKPNLH  | HLAllergen3 (API81354, <i>Hemiscorpius lepturus</i> )                           |
| LaCRVP2                            | MFIPLALLTAIRLSLRDRCCYAEFLANPSVWVWETETVCPTTPTYAGSVKSKRNANPGTPIPLSDQDKMEIVNEHNKYRGQVSP<br>PAANMRYMIYNEDVAYAAQLWANGCQFRHGRPQGSKFQKLVGQNIYKGPSGSYSFYMLRWHNEVRDFDMKSQQCNATMC<br>GHYLMVWVAESFLIGCGQSHCRGKRRSYNLFVCHYYKAFESFHPYKVGPRCSMCDAEAGGFYNNCTVSKEDCEREGWPC  | HLAllergen1 (API81352, <i>Hemiscorpius lepturus</i> )                           |

|         |  |   |
|---------|--|---|
|         | ECNLKCHNCGILDESTCTCKCPPGWDYQDCSQNCSDSSDYCGKEDGFEGVWVCEMLEDGYYKTHYCRKMCETCEVITEGN<br>KEKTCGGELCDKGYVLDNSNCNCRRLCPGPECYFTYEDNGVAYRVNTSLLTVIIAGIYALWQGQEPKPG  |   |
| LaCRVP3 | MEKNVLWLIVLHLSLIWVKSQRDVGIAKFTGNLSSAWVHKL RVDYRLKRRVARLASMMNDSRLEVIRLHNL YRSMVAPPAA<br>DMEYMAWDDRLASLSQQWAECKWRHGNPRHDFPTGLGQNL YRGSVRSVALAIRLWYEEHV DRYRHNLS CNPKKQCGHY<br>TQMVVSKTHLVGCGVKNGCWKGFKHYIVCNYP SHYKGEKPF EIGRPCSLCNSTKSGLCWNKSCVSR SQCEEYK LDCSCD<br>LICHNCGKLDREKCTCICKDGWKGVD CSEPCVDTMEDCSLYHC IYHEYSRNHPCLKSCNVCKPVNADDLRNSCCDGVSCPH<br>GYVLDLADIPCECKPLCPGPKCGSLLHGPYFTLMLFVLLLLKCSAL   | HLAllergen2 (API81353, <i>Hemiscorpius lepturus</i> ) |
| LaCRVP4 | MEWTFVCSIMLSFAPLTWGKTQFETERINVSYSWVHYGGMSRRARATSMMKDPDKLEITRLHNSYRSMVSPSAVDMEYMEW<br>DDRIASVSQQWADRCTWKHSDTAIADFPDGLGENLYRGWSSSPAYAMNLWYSEYTHYDIQNTSCKPGKVC GHYTQM VWS<br>KSRLVGC GVKEGCWRDYRYIVCNYSPPGN YKGEKPYQIGRSCSHCHSGSGLCSNKSCVDRSQCDKYNLDCSCDLVCLNC<br>GELNRHSCTCKCKEGWKGVD CSEPCQDAQENCLVSACSYYERWPRGSHPC EKT CNVCKSVTPDSVQNTCCDGVTCPPGEI<br>LDLSEPCCKKLCSGPKCQSSLHEPHSLFLLVAMSIFLRCYAR   | HLAllergen2 (API81353, <i>Hemiscorpius lepturus</i> ) |
| LaCRVP5 | MAAVAVALVVLWITVTSGSANNDTCAERYTNITPEHTMCKSTNENCTFVRSSGEVFEEQLLRTHNLIRNSIRKYV GKKYHLATN<br>MKLMVWDD ELYEMARLHSLQCVEEPCDCLCHQIGDFPVEQNF AVKTFKSSEVDGNGPIRRLQAVIEEWA AELRSYDCD VVKV<br>FRNTEGLPTNWTNIFRATTMLVGCASMTFLTDEPGTFKEVYVCNYGPANLTEGEEIYRTGRKPCSECEDEDEGCDTEFKHL CFP<br>ADMEEENIPEETELHNTFARNMVTKKFPRQRRRYLWNTDVARSYLDRRTENWRRTGGGV TGSYPDYRTGNWNGT GEGVTR<br>SSHTYQCKRKSETSQLSESSILVMEQQGF  | HLAllergen7 (API81358, <i>Hemiscorpius lepturus</i> ) |
| LaCRVP6 | MEIFLAIPCLLTAFLPSISNERCSDSFGNYDQALFREGTRDES VQISWWTTTPISKETGDKTRTSEEKECEPELYQRYSRNHTFC<br>QVSNCDIIRKGVTEEDKNIILEFHNSLRSKLASGMEKRYCSLPSAANMMQIEWDDELA AVAEAAELCVYGHDRGKRAVESFS<br>VGQNLMLYGGDIKRWGDADGWYKEEVCFYSPEKNSPFRSGIYGHFTQVTWATTWKIGCGFAS YRKNKGKVEALYTCNYGPS<br>GNVREGRHYIVGEPSCQCPPNTECSTEDPGLCKSKTCDGPQMRPPSEDFILFCDFSHEDSEECNKVKVNGSREFSTRHIYT<br>GNYKT VVLNAGESITIDLGAQNDGGICTFVYSRFGPNNAKDAPGSVMEIKYESPNILPVPPRTIGPYGPTFFMAGTHMSYHGE<br>LQNTLTLRALEGAEPQYFDIKMWGIRKGDCLMSLESD    | HLAllergen2 (API81353, <i>Hemiscorpius lepturus</i> ) |
| LaCRVP7 | MEIFLAIPCLLTAFLPSISNERCSDSFGNYDQALFREGTRDES VQISWWTTTPISKETGDKTRTSEEKECEPELYQRYSRNHTFC<br>QVSNCDIIRKGVTEEDKNIILEFHNSLRSKLASGMEKRYCSLPSAANMMQIEWDDELA AVAEAAELCVYGHDRGKRAVESFS<br>VGQNLMLYGGDIKRWGDADGWYKEEVCFYSPEKNSPFRSGIYGHFTQVTWATTWKIGCGFAS YRKNKGKVEALYTCNYGPS<br>GNVREGRHYIVGEPSCQCPPNTECSTEY PGLCKSKTCDGPQMRPPSEDFILFCDFSHEDSEECNKVKVNGSREFSTRHIYT<br>GNYKT VVLNAGESITIDLGAQNDGGICTFVYSRFGPNNAKDAPGSVMEIKYESPNILPVPPRTIGPYGPTFFMAGTHMSYHGE<br>LQNTLTLRALEGAEPQYFDIKMWGIRKGDCLMSLESD   | HLAllergen2 (API81353, <i>Hemiscorpius lepturus</i> ) |
| LaCRVP8 | MDLLFAISCLLAFLPCICNKRCNSIYGKYDQGTLSKGARDETFLSSWRNVIPINIERGEKTQF SERKECEPELYQRY S ADHTFCK<br>KSTCSIIQKGVTEDEKNTILKFHNSLRSKLASGKEARYSKTPLPSAANMMQLEWDNELAAVAEAAELCLYDHDANEQRAVEN<br>FPVGQNL MQYNGDIRKWDADMWYKDEVCFYSPQYNSPFGDFGHFSQVTWATTWKIGCGFTSYRKDGSEKALYTCNYG<br>PAGNVPGGRHYIVGKPCSQCPPNTECSTEY PGLCKSKTSDGPQMKRPSEDFILFCDFSQADPEECKVKVSGSREFSTRHI<br>YTGDYKT VVLNAGESISIDVGKAQNTGGICPFVYARFGPNNAKDPVGSVVEIQFSAPNIVPMPPSTVTPLG SFFVAGTHMMYD<br>GELQSVLTLKAEQGA KPQYFDVKAWGV RKGSCGTS LGPK | HLAllergen2 (API81353, <i>Hemiscorpius lepturus</i> ) |
| LaCRVP9 | MEVTSRPVTEANPVIQPLLTWKWTHLYICARKRIRAIINLHFLT VETANMNLTLVVSILCLALFTCQVVYSQRCEIYQRFSEDH<br>TYCKHSTCQVIKSGVTDQDKKIILDMHNSYRNKVALGQEDTPQRQPPAANMLQMEWDD ELARIAQA HANLCKFEHDSPDQRQ  | HLAllergen1 (API81352, <i>Hemiscorpius lepturus</i> ) |

|          |  |   |
|----------|--|---|
|          | <p>VENFNVGQNLFISSMMTQVIDWNKTAMWYTWEIKHYYPQYREPFASGPYLHLSQMIWADTWKVGCGVAVYYDNNERRDKVLY<br/>         TCNYGPGGNQIGQKVYTAGKPCSQCCKNTQCSSEYKGLCKSRTPDGPQQDTTRNPDDFLLYCDFSNNEEDRACKNVQISGLR<br/>         QFETRKIYGGYKIAILKGGESITFKLGKAKDSRGICPFYIGSFGPNRAGDAKQSAVSIGFAASGLIFGDPIKIDYGSDFWPIGM<br/>         HMQYDQEMESTIKLEAYPGAPPQYFKIKAFGIGKCKPKF</p>   |   |
| LaCRVP10 | <p>MDFLLAISCLLAFLPCNSNHLCELYGEYDEDSDESDYPSSEWEEIPTDEERGEKESQISERKECEPELYQRYSTNHTFCKESTC<br/>         DIIRRGITEEDKNTILEFHNSLRSLKSLASGKEARYSQTPPLPSAANMMQMEWDDLAAVAQAHAELCIFNHEPDDQREVENFPVG<br/>         QNLMQFDYDIKSWESAIEWYKEEVCFYSEEYNPFNSGIFGHFSQLTWATSWKVGCGFASYRVNGSEKGLHTCNYGPPGNV<br/>         AGGRHYIVGEPSCSRCPNTECSTEYPGLCKSKTSDGPMKRPSEDFILFCDFSQEDPEECDGVKVNRSREFSTRHLYIGDY<br/>         KTVVLNAGESISIDLGAQNTGGICPFVYARFGSNNAKDPAGSVLEIQFDAPNMWSMPPPIRVNPNYGDSFQVAGVQMMYDDEL<br/>         QSILTFKAEAGAKPQYFDVKAWGIRRGSCETSLDPEDEN</p> | HLAllergen2 (API81353, <i>Hemiscorpius lepturus</i> ) |

**Insulin-like growth factor binding protein**

|       |  |   |
|-------|--|---|
| LaVP1 | <p>MGKFLLIALFLFGVTVSALGLSCRPCGTYQCPPLPRCPVGVKDACFCCQVCAKGLNERCGGPWNISGRGRLKCFKQAQ<br/>         DAIGVCRKV</p>           | Venom insulin-like growth factor binding protein-1<br>(ABR21044, <i>Mesobuthus eupeus</i> ) |
| LaVP2 | <p>MALRFCFITLLLLGVILGAMTLRCRQCCTYECPPAPENCPVGKVKDICNCCDECGKNGECCGAWDMYGKCGKGLRCFKEP<br/>         VEGDPFNAKGTCR</p>     | Venom insulin-like growth factor binding protein-1<br>(ABR21044, <i>Mesobuthus eupeus</i> ) |
| LaVP3 | <p>MWFRLVLFVLTYSIYSLSCPCHELDLEEFSGPPKDCPLGLTLDACACCQVCFLETEGEVCGGPWDVNGKCGAGLTCVKPPG<br/>         QSDFVFDQSDGVCKKQ</p> | Venom insulin-like growth factor binding protein-1<br>(ABR21044, <i>Mesobuthus eupeus</i> ) |

Table S3 Comparison of inhibition of HCV infection between pretreatment and post-entry treatment with LaPLA<sub>2</sub>-1

| LaPLA <sub>2</sub> -1<br>(ng/ml) | Inhibition (%) |                      |
|----------------------------------|----------------|----------------------|
|                                  | Pretreatment   | Post-entry treatment |
| 100                              | >99.9          | 8 ± 6                |
| 10                               | 92 ± 1         | <0.1                 |
| 1                                | 16 ± 23        | <0.1                 |
| 0.1                              | <0.1           | n.t. <sup>a</sup>    |

<sup>a</sup> n.t., not tested.

Table S4 Cytotoxicity of LaPLA<sub>2</sub>-1.

| LaPLA <sub>2</sub> -1 (ng/ml) | Cell viability (%) |
|-------------------------------|--------------------|
| 1000                          | 79                 |
| 100                           | 100                |
| 10                            | 100                |
| 1                             | 100                |

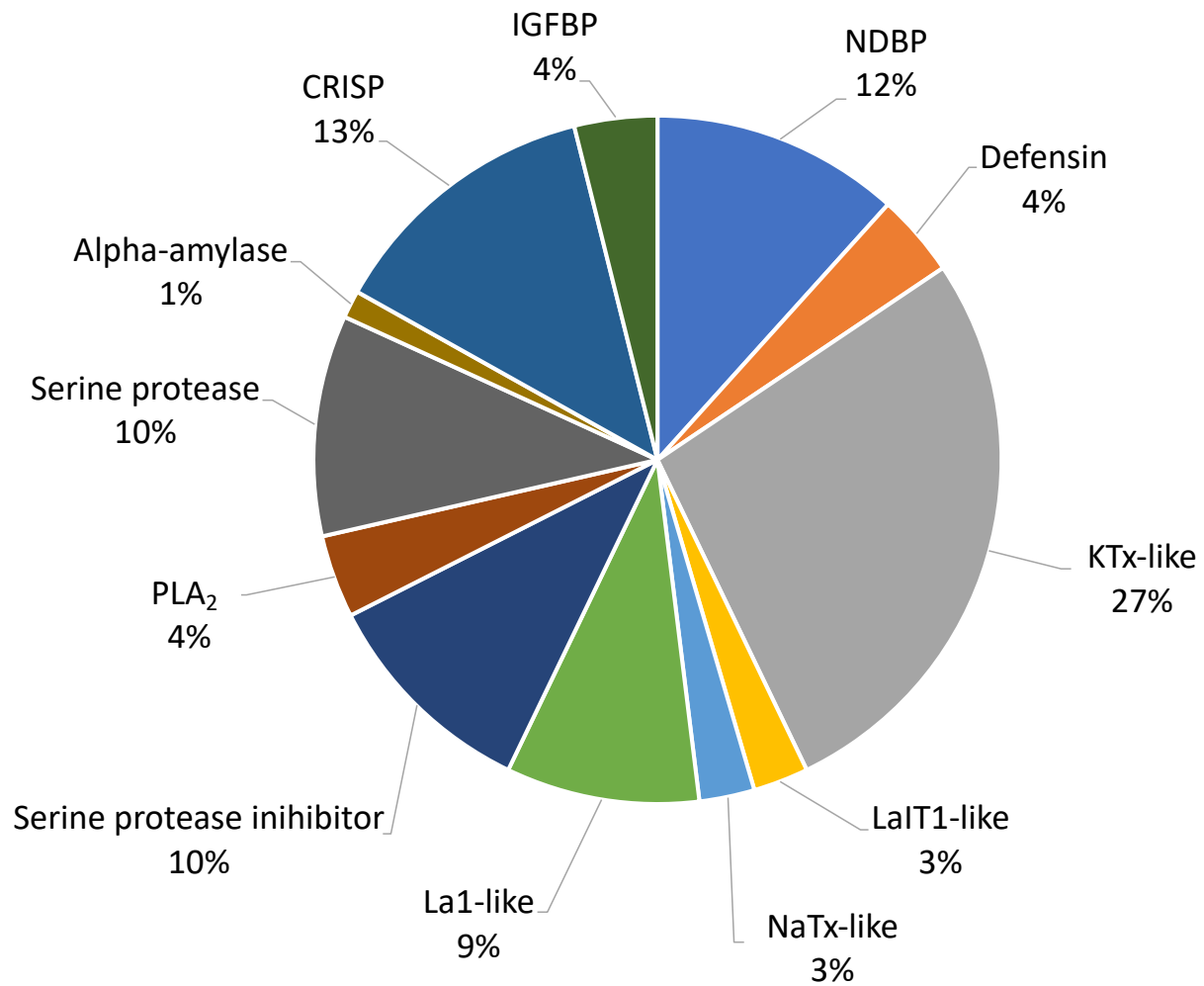


Figure 1. Proportion of the components identified by venom gland transcriptome analysis



(a) NDBP

|                  |   |           |
|------------------|---|-----------|
| <b>LaNDBP2-1</b> | MNIKVVLVVCLITLLVTEQVEGGWFSRIKSLAKKAWKSNLAKDLRKMAGKAARNYAARKVNLVNSPEEQVQL--DNLLRYL--D      | 100 (%Id) |
| <b>LaNDBP2-2</b> | MNGKVLVVCLIVAMLVMEPAEAGIWGWIKKTAKKVWNSDIANQLKNKALNAAKNYVAEKVGATPAEAGQMPFDEFMDIYY-S        | 37        |
| <b>Vejo vine</b> | MNAKTLFVVFLIGMLVTEQVEAGI <u>WSSIKNLASKAWNSDIGQSLRNKAAGAINKFVADKIGVTPSQAASMTLDEIVDAMYD</u> | 42        |
| <b>LaNDBP3-1</b> | MQYKTFVLVIFLAYLLVTEEAQAQFWWALAKGAALKLLPSVVGAFTRK-KREIEKIFDPYQSSLDLEMERFLRQLQ              | 100       |
| <b>LaNDBP3-2</b> | MKLRTLMLVIFLAYLIVTDEAEAFWGF <del>LAKAAKLLPSLFSSKKEKEKREIEHFFDPYEKELDSELDQLLYELQ</del>     | 56        |
| <b>Heterin2</b>  | MQYKTFVLVIFLAYLLVTEEAALAF <u>WGALAKGALKLIPSLVSSFTKKDKRALKNIFDPYQKNLDLELERLLS</u> QLQ      | 75        |
| <b>LaNDBP4-1</b> | MKIQLAILVITVVLQMQLVQTEAGFWGKLWEGVKNVIGKRGLRNKDQLDD-LFSDLSADADAKLLREMFK                    | 100       |
| <b>LaNDBP4-2</b> | MKIQLAILVITVVLQMQLVQTEASFWGKLWEGVKSAGKRGLRDVDQMDD-LFSDLSADADAKLLREIFK                     | 90        |
| <b>LaNDBP4-3</b> | MKNQFVILLLLAIVFLQLFSQSEA-FLSALWGVAKSLFGKRGLKNLDQLDD-LFDGEVSEADLDFLKELMR                   | 48        |
| <b>LaNDBP4-4</b> | MKAQIVLLVITVVLQMFAQSEAGFWGKLWEGVKSAGKRGLRNLDQFDDELFDSDLSADADAKLLKEIFK                     | 80        |
| <b>OcyC2</b>     | MKTQFAILMIAVVLQMQLVQTEG <u>GILGKIWEGVKS</u> LIGKRGLKKLDQLDD-TFSDLSADADVLLREMFK            | 78        |
| <b>LaNDBP4-5</b> | MRLVSLTPLFLILLIAVDYCSFP-FLLSLIPSAISALKKLGKRSTDFQRQLDFQRRYLNSDLDFDLDELEEFLDQLPDY           | 100       |
| <b>VpAmp1.0</b>  | MKLINLVPVFFVLIIVVDYCHSL <u>PFLLSLIPSAISAIKKIGKRSVESQRYVDLNR</u> ----DLEQDLQELQDFLDQISEH   | 58        |

(b) Invertebrate defensin

|                    |  |     |
|--------------------|--|-----|
| <b>LaDefensin1</b> | MKAIATLLLLILVAFSVLEFGIVDAGFG <u>CPFNRYQCHSHCQ</u> SIKRRGGFCAGTFRTTCTCYKSK----- | 100 |
| <b>LaDefensin2</b> | MKAIATLLLLLVAFSILEDGIVDAGFG <u>CPFNRYQCHSHCR</u> SIGRRGGYCSGPFRTTCTCYK-----    | 85  |
| <b>LaDefensin3</b> | MKAIATILLLLAAFSILEFGIVGAGFG <u>CPHNRYQCHSHCQ</u> SIGRNGGYCGGTFRTTCTCYNSGGPTSSP | 74  |
| <b>AbDef-1</b>     | MKTIVLLFVLALVFCTLEMGVVEAGFG <u>CPFNQGRCHRHCR</u> SIGRRGGYCRGIFKQTCACYRK-----   | 55  |

Figure 2. Multiple sequence alignment of NDBPs (a) and invertebrate defensin peptides (b) identified in this study and comparison with their similar peptides. Mature regions that were previously reported are underlined. Cys residues in the reported and putative mature regions are shaded in yellow. %Id represents the percentage of sequence identity.

(a) Alpha-KTx

|                     |   |           |
|---------------------|---|-----------|
| <b>La-alphaKTx1</b> | MNAKFIYILLTAVMFALYEASVPPNIPCQVTNQC PKPCREATGRPNKSCINGRC KCYG-----     | 100 (%Id) |
| <b>La-alphaKTx2</b> | MNTKFVFLLLVISTLMPTFDAS-AEDISCSSSKECYDPC EEETGCS SAKCVGGWCKCYGCRG---   | 41        |
| <b>La-alphaKTx3</b> | MNRNFVFLLLLVITLMPMLDAA-TEDINC DNWRDCLKPC KDETGCPNSKCEEGNCLCYGCNRLTV   | 42        |
| <b>Urotoxin</b>     | MNAKLIYLLLVVTTMMLTFDTTQAGDIKCSGTRQWGPCKKQTTCTNSKCMNGKCKCYGCVG---      | 48        |
| <b>La-alphaKTx4</b> | MNKKFIFLLLVVTTLMPMFDA-ATEAISC SNPNDCREPC KKTGTGCSGGKCMNRKCKCHRCNG     | 100       |
| <b>OcKTx2</b>       | MNAKFIYLLLVVTTMMLLPDQTQAEVIKCRTPKDCADPCRKQGTGCPHGKCMNRTRCNRRC-G       | 61        |
| <b>La-alphaKTx5</b> | MNAKLVCI VLL-TAVMFAPDEASLPPIRIPC YVSKDCRKPCLYLTGT PRSKCINRRC KCYG---- | 100       |
| <b>Hemitoxin</b>    | MNTKFIFLFLVVT TMLLFDTTAVEA--IKCTLSKDCYSPCKKETGCPRAK C INRNC KCYGCSG-  | 48        |
| <b>La-alphaKTx6</b> | MNKPFCAIFLVVLMFAVSVLPAES--TGGCPV-DSLCKSYCKSNKFGTEGKCDGTS---CKCAIG     | 100       |
| <b>La-alphaKTx7</b> | MNKLACYILICVMVSLFKVPVAEGI-SAGCPLTAKLCTIYCKKHRFGREGKCI GPTRFRCKCYV-    | 44        |
| <b>LmKTx8</b>       | MNKVCFVVVLVLFVALAAYVSPIEGVPTGGCPLSDSLCAKYCKSHKFGKTGRCTGPNKMKCKLV-     | 49        |
| <b>La-alphaKTx8</b> | --MRLV I ILLM TTVLAVGAPLGGAKCSSSTQC TRPCRYAGGTHGKCMNGRCRCY--G         | 100       |
| <b>St20</b>         | MKMSIV I ILLLFTCL IATNGA--SGTKCSGSPECVKFCRTKGC RNGKCMNRSCRCYLCS       | 49        |
| <b>La-alphaKTx9</b> | MELKYL VLLAVTCLVSCQDNSLLPSGSCSRTGICMESCAPFLYQPKYHRRCPAGYVCC TLIY      | 100       |
| <b>Kbot55</b>       | -----AGSMDCSSETGVCMKACSERIRQVENDNCKPAGECICTT--                        | 39        |

(b) Beta-KTx

|                            |  |     |
|----------------------------|--|-----|
| <b>La-betaKTx1 (LaIT2)</b> | MAKHLIVMFLVIMVISSLVDCAKKPFVQVRVNAASKAYNKLGKGLAMQSQYGP I I SNMCEDHCR RKKMEGQCDLLDCVCS                       |     |
| <b>La-betaKTx2 (LaIT3)</b> | MQAQFTVLLLLLVLTLCSCGGILREKYFHKAADALTSNIPIPVVKDVLKSAANQMIRKIGKVQQA CAFNKDLAGWCEKSCQEAEGKKGYCHGTKCKCGKPIDYRK |     |
| <b>La-betaKTx3</b>         | MDTKLSILVFLCVVVIASCSWI SEKRIQKALDEKLPKGF IQGAAKAIVHKFAKNQYGC LADMDVKGSCDRHCQETESTNGVCHGTKCKCGIGRVY         | 100 |
| <b>SC11</b>                | MNTKFITVLI FLGVI-VVSYGWITEKKIQKVLDEKLPNGFIKGAAKAVVHKLAKSEYGCMMDISWNKDCQRHCQSTEQKDGICHGMKCKCGKPRSY          | 60  |

(c) Kappa-KTx

|                     |  |     |
|---------------------|--|-----|
| <b>La-kappaKTx1</b> | MKPSTSAYALLLVLTFGIIT--SGVFAVPMDEENTFEVEKRGNSCMEVCLQHEGNVAECEKACNKG         | 100 |
| <b>La-kappaKTx2</b> | MKPSTSAFILLLVLTFGIIT--SGVSAIPMDEENTFEEQKRDSACVEVCLHHEGNVAECEACKKS          | 78  |
| <b>HeTx203</b>      | MKTSGT VYVFLLLLAFGIFTDISSACSEQMDDEDSYEVEKRGNA CIEVCLQHTGNPAEC DKACDK-      | 59  |
| <b>La-kappaKTx3</b> | MKLLPLL-VILII CALMANEAFCDQGARER-SENLED-TRDLVQKPCRIVCSENMR--KCIRRC TL--G--R | 100 |
| <b>La-kappaKTx5</b> | MKLLPLLVLIVCALLPNEAFCDQSAVER-SESLEEVSREIVKRSCKRVC SGTRRTKKCMQKCKSQPG--R    | 58  |
| <b>HeLaTX1</b>      | MKLLPLL FVILIVCAILPDEASCDQSELERKEENFKDESREIVKRSCKKCESGSRRTKKCMQKNREHGHR    | 47  |
| <b>La-kappaKTx4</b> | MKPSSFAIALILVFLGFTNAVSGEYAESI---SGDRME---RAERAGCRIRCLQFTDDFEKCRKLCG--      | 100 |
| <b>PcavC10</b>      | MK-SSLVVASLLI LFLVVSINDYTSVYAQSTHEESGSKMERRARIKRAGCVIKCLQFTPELEKCRKLCGLK   | 50  |

(d) Delta-KTx

|                     |  |     |
|---------------------|--|-----|
| <b>La-deltaKTx1</b> | MASQFLLCIVLIAVNPLVYSKG-GRLPPETGLYAYFERYYYDPSSNNCKMFVYGGCGGNSNPFVSKKACLARCAN---       | 100 |
| <b>BmKT-2</b>       | MNVIITVVGII LSVVCTISDAEGVDC TLPSTDTGRCKAYFIRYFYNQKAGECQKFVYGGCEGNSNFLT KSDCCQCS PGKC | 42  |

Figure 3. Multiple sequence alignment of KTx peptides identified in this study and comparison with their similar peptides. Mature regions that were previously reported are underlined. Cys residues in the reported and putative mature regions are shaded in yellow. %Id represents the percentage of sequence identity.

| (a) DDH                             |   |           |
|-------------------------------------|---|-----------|
| <b>LaDDH1 (LaIT1)</b>               | MNFATKVFLLLLAVAVIAIVAGEEDDSWFEQNEESDTERDFPLSKEYETCVRPRKCQPPLKCNKAQICVDPKKGW-----  | 100 (%Id) |
| <b>LaDDH2</b>                       | MNCAIKVSFLLLAITVIFSVAGGEDNSFEQREENDTERDLPLSKKHESCVRPRKCRPPLRCNKAHICVESKKGWRIPVISWVSKTKIMFSE   | 71        |
| <b>Phi-LITX-Lw1a</b>                | MNFATKVSLLLLAIIVIVIVEGEGDSWFEEHEESDTERDFPLSKEYESCVRPRKCKPPLKCNKAQICVDPNKGW-----   | 84        |
| <b>OcyC10</b>                       | MNFATKIVILLLLVAALILAVTSEKGDSSDDNEAKETEDELPLSDFYGCVRPKCKPHLKNAAQICVFPKTGR-----   | 56        |
| (b) NaTx                            |   |           |
| <b>LaLAP1</b>                       | MNTGEHFASLIIFLLLLGENPCLDGGWPMRIDGNYLCCYYEEKPAELYCKRACKLHKASQSSCSYHWKYMSWYCCEDLK-----KGYTRDRGLKKGGGHQFSES  | 100       |
| <b>LVP-1-alpha</b>                  | MNI-KLFCFLSILISLTGLSLSGDDGNYPIDANGNRYSC--GKLGENEFCCLKVCKLHGVKRGYCYF-----FKCYCELLKDKDIQFFDAYKTYCKN-----SRI   | 26        |
| <b>LaLAP2</b>                       | -MLMVIYIATLIPLILQGECAKDD---HPRNFEGNCCYRCKYPDKSGYCEAICKMHKAETGYCSRSNLFCCYCKGIEDKYVS-----ARDFLEP---   | 100       |
| <b>BmLVP1-alpha</b>                 | MMKFVLFGMIVILFSLMGSIRGDDDPGNYPNTAYGNKYCTILGENEYCRKICKLHGVTYGYCYNRSR--CWCEKLEDKDVTIWNVAVKNHCTNTILYPNGK   | 33        |
| (c) Ascaris-type protease inhibitor |   |           |
| <b>LaAPI1</b>                       | MKS--WTYRLCFLILFLVCV--NCT-RPVLSPEEC <sup>C</sup> TRPGEFFTTAGSYC <sup>C</sup> PLTC <sup>C</sup> DNYKN--P-PIIC <sup>C</sup> SLIGIVG <sup>C</sup> EC <sup>C</sup> SPELVRDEERSGN-CVDTSD <sup>C</sup> CTED-----                      | 100       |
| <b>LaAPI2</b>                       | MKG-----FAFLVLTFFVVF-----GDKEQECEDPNAEFRRONTAC <sup>C</sup> PITCANMDN--P-PNIC <sup>C</sup> TLQCVIGCACKEGYKND-DGL-CVHPEGC-----   | 33        |
| <b>LaAPI3</b>                       | MKA--LLLLSFVVIH--SAKSQEDLGGDEHAQSC <sup>C</sup> LLPNEVWDKCGPSCPPSCIGVIE--P-GTLC <sup>C</sup> STECTPG <sup>C</sup> FCREGLV <sup>C</sup> RTK-RGS-CIPPKACRNERETKL  | 25        |
| <b>LaAPI4</b>                       | MKGSKPLCFLYLVLVLLWTSV--KCT-RWASSSEEC <sup>C</sup> TRPGEAFTSC <sup>C</sup> GTDC <sup>C</sup> PITCANYEN--P-PEFC <sup>C</sup> NYMCVIG <sup>C</sup> ECTSGLV <sup>C</sup> RDEGSGN-CVNPSQCGP-----                                     | 51        |
| <b>LaAPI5</b>                       | MKR--NLVLLAFVLLLFSGSIFEKCSAQRGGADRR <sup>C</sup> RRPGEVFMNCGPSCPLTC <sup>C</sup> DNYQN--P-PTV <sup>C</sup> TLQCVIG <sup>C</sup> FCRRGLV <sup>C</sup> RDTRRGG-CVRPSQ <sup>C</sup> RR-----  | 42        |
| <b>LaAPI6</b>                       | MKR--NLALSALFVLLFCSALDNCEAQRGGYDRT <sup>C</sup> QLEGEVFT <sup>C</sup> RCGTAC <sup>C</sup> PLTC <sup>C</sup> DNYRN--P-PEV <sup>C</sup> TLQCIIG <sup>C</sup> CVCGRGW <sup>C</sup> KDTRRGR-CVRPSQ <sup>C</sup> RR-----             | 40        |
| <b>LaAPI7</b>                       | MKS--NLVLFVAFVLLLFCSVLEICTAQRVVDRS <sup>C</sup> RGAGEVFT <sup>C</sup> RCGTAC <sup>C</sup> PLTC <sup>C</sup> DNYRN--P-PRF <sup>C</sup> TRQCIIG <sup>C</sup> CACRRG <sup>C</sup> WKATRGG-CVRPSQ <sup>C</sup> RR-----              | 40        |
| <b>LaAPI8</b>                       | MAKT-----LAFGVVLCMFVLAQSAPQYPGTFG-C-DEDKQFV <sup>C</sup> RLPP <sup>C</sup> CVTCKSILN <sup>C</sup> TTP-CTLLLP <sup>C</sup> RCTPG <sup>C</sup> CG <sup>C</sup> RRGKILDN-AGK-CVFPAD <sup>C</sup> RRG-----                          | 22        |
| <b>SjAPI</b>                        | MKW--GALLCIFGFLAFCSVLDRGLGWIPDIWQK <sup>C</sup> SSKNEEFQ <sup>C</sup> CGSS <sup>C</sup> PETCANHKN--PEPKS <sup>C</sup> AAVCFV <sup>C</sup> GV <sup>C</sup> CKPGFIRDDLK <sup>C</sup> GSICV <sup>C</sup> KPED <sup>C</sup> SK----- | 34        |

Figure 4. Multiple sequence alignment of DDH (a), NaTx (b), and Ascaris-type protease inhibitor peptides (c) identified in this study and comparison with their similar peptides. Mature regions that were previously reported are underlined. Cys residues in the reported and putative mature regions are shaded in yellow. %Id represents the percentage of sequence identity.

```

La1      MG-----GTLKHLVVCLIVVCSLCLGFG-----ESIAGRF-IVPLGQQTVDQRDCALYKCVNYNKKFALETKRCATVNL-K-SGCKTVPGGAGAAFPSCCP-MVTCKG----- 100 (%Id)
La1-1    MK-----HLHAAVLLVCLISICALPSLTLGAG-----ESKVGSL-VIPVGQKKFKPSCAEYECSTEFNRVLLKAITCATLNT-KGKGCKSVPGKSPNSFPDCCP-TILCRGEQWNH----- 42
La1-2    MK-----IVCTIVPLVF-----ACIANAHVLTE-----RTRTHTGVILKNGEWADPNHCSIYRCTIYSGEAELQGLTCATYRV-P-PNCEFVVRGRGKF-YPSCCP-TVMCKP----- 25
La1-3    MA-----LRFVLAFLLPCLVLGSNEPAKFISYKNDMLGPLVEGKCKVGNDKMIEQGGTWYRDDYCEKIYCLRTGTLGHMEVWGCAPVAPLN-PNCTVVHHSGL--YPNCCSGEIVCEENPDTKKSDVEMAEIIRALLQSERK 17
La1-4    MF-----NIVTITLLWSCTCIALCHSYG-----ETCQAGEL-TIPLDNEKQDPEACTLYKCTMFAGRVVLTNTLTCAPQEP-R-RGCRNVDSPVELPFPDCCP-LVVCNVQPLGSK----- 32
La1-5    MR-----TLVPAVFLALIVAAMASHKDPYH-----RNCPIGNK-DLSDGEWADQQRCVKYKCQIRGPDALLLTRCPSVGIYPPDKCREIAGKGN--FPDCCP-KLOCD----- 28
La1-6    MSRADKAFVGTLLIAIFLVCSLTNAYSSLKRQYGS-----APCVDHLGSRKFDVWYDNESCEEHTCIKYRGIPHVQIYCIAAVA-S-PGCELVKGSGS--YPDCCE-EEIC----- 19
La1-7    MKTWEARFYIFLVALVTITFVESYVYLVPQDPGA-----VVCIGKDRVSHKPGDVWYDDSKCERLTCGHSSGGLVIDGAGCGSISV-Q-DGCKLVPGVGS--YPSCCP-SPVC----- 19

```

Figure 5. Multiple sequence alignment of La1-like peptides identified in this study. Mature regions that were previously reported are underlined. Cys residues in the reported and putative mature regions are shaded in yellow. %Id represents the percentage of sequence identity.

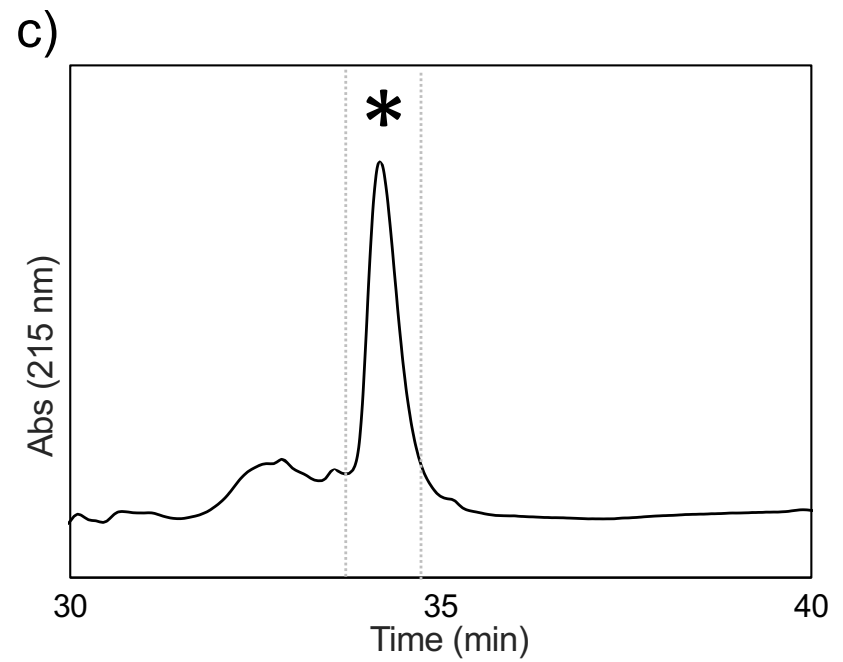
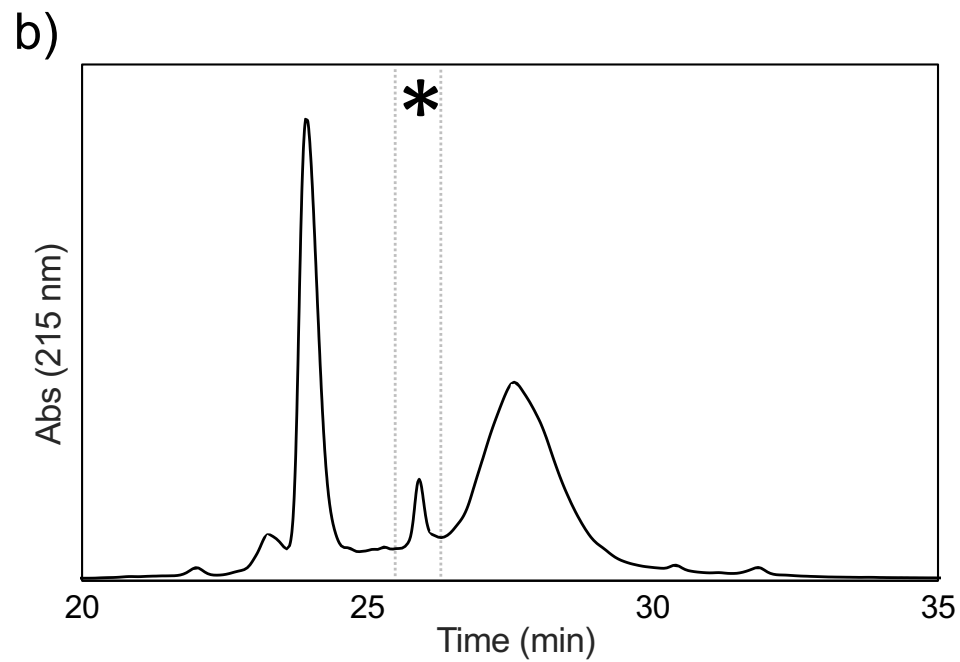
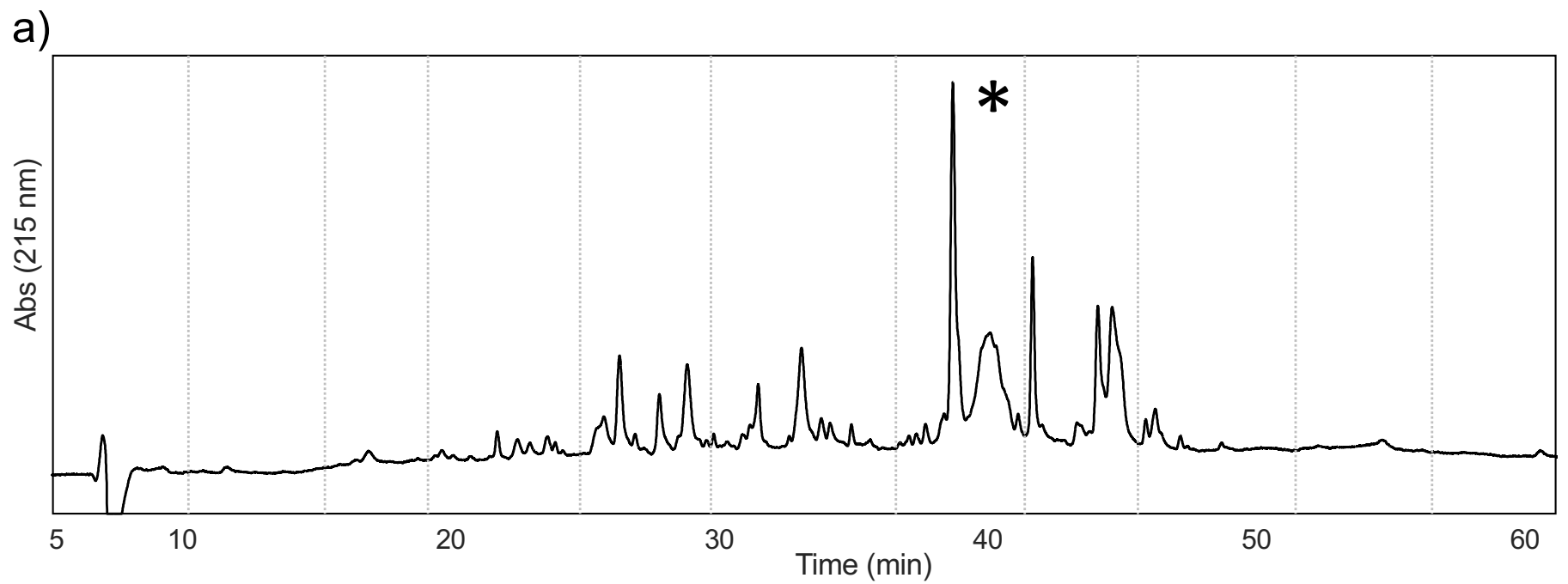


Figure 6. HPLC purification of an anti-HCV component from the venom. (a) First separation using a C4 column. (b) Second purification using a C18 column. (c) Final purification using a C18 column. Asterisks indicate fractions showing anti-HCV activity.

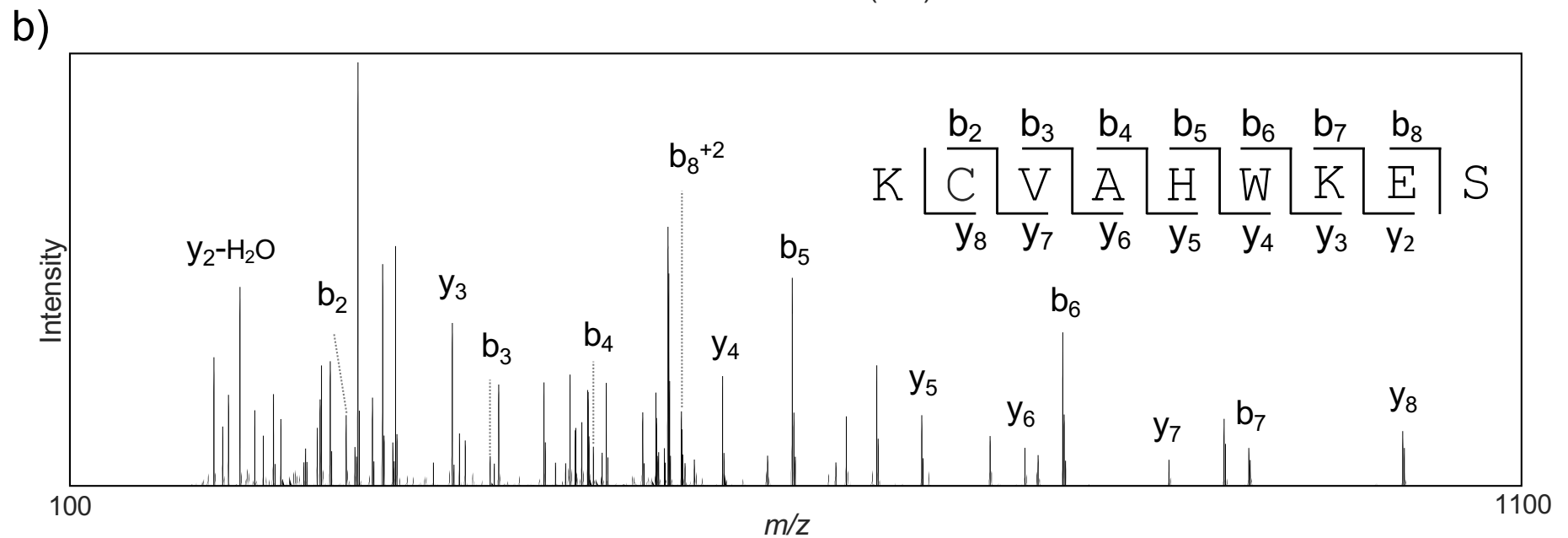
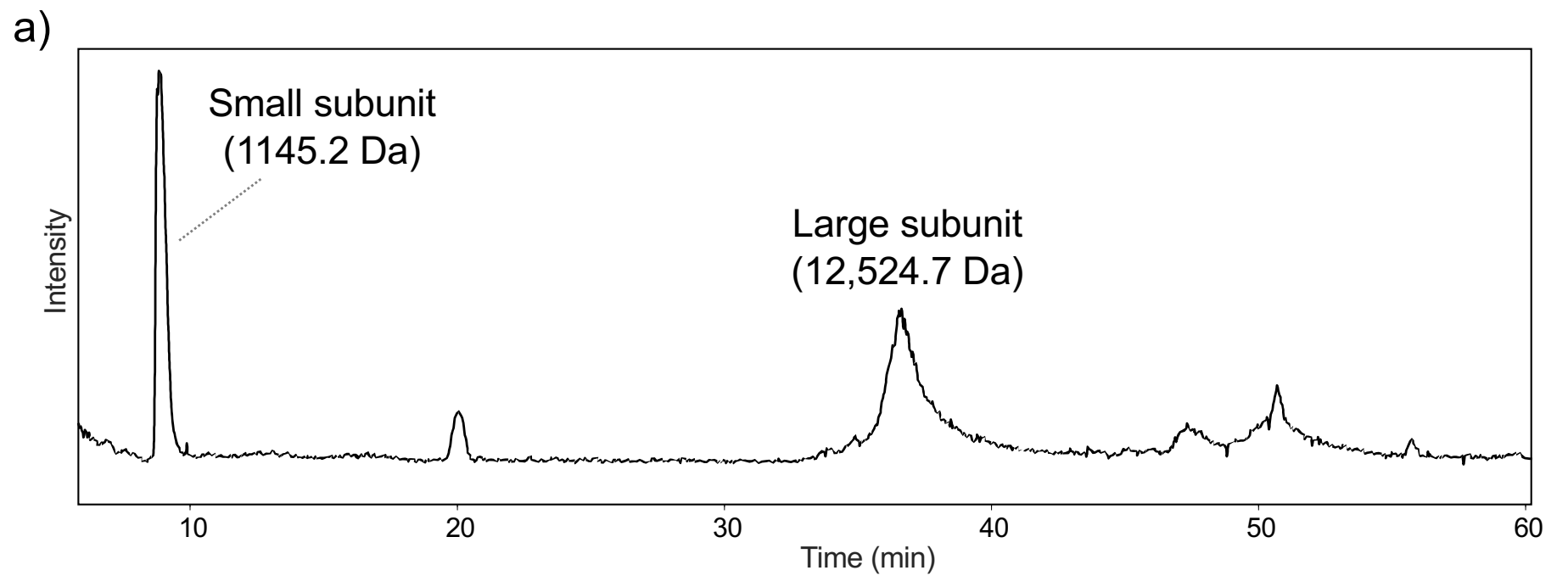


Figure 7. LC/MS analysis of the anti-HCV component after reduction/alkylation reactions. (a) TIC chromatogram of the reaction mixture. (b) Product ion spectrum of the small subunit.

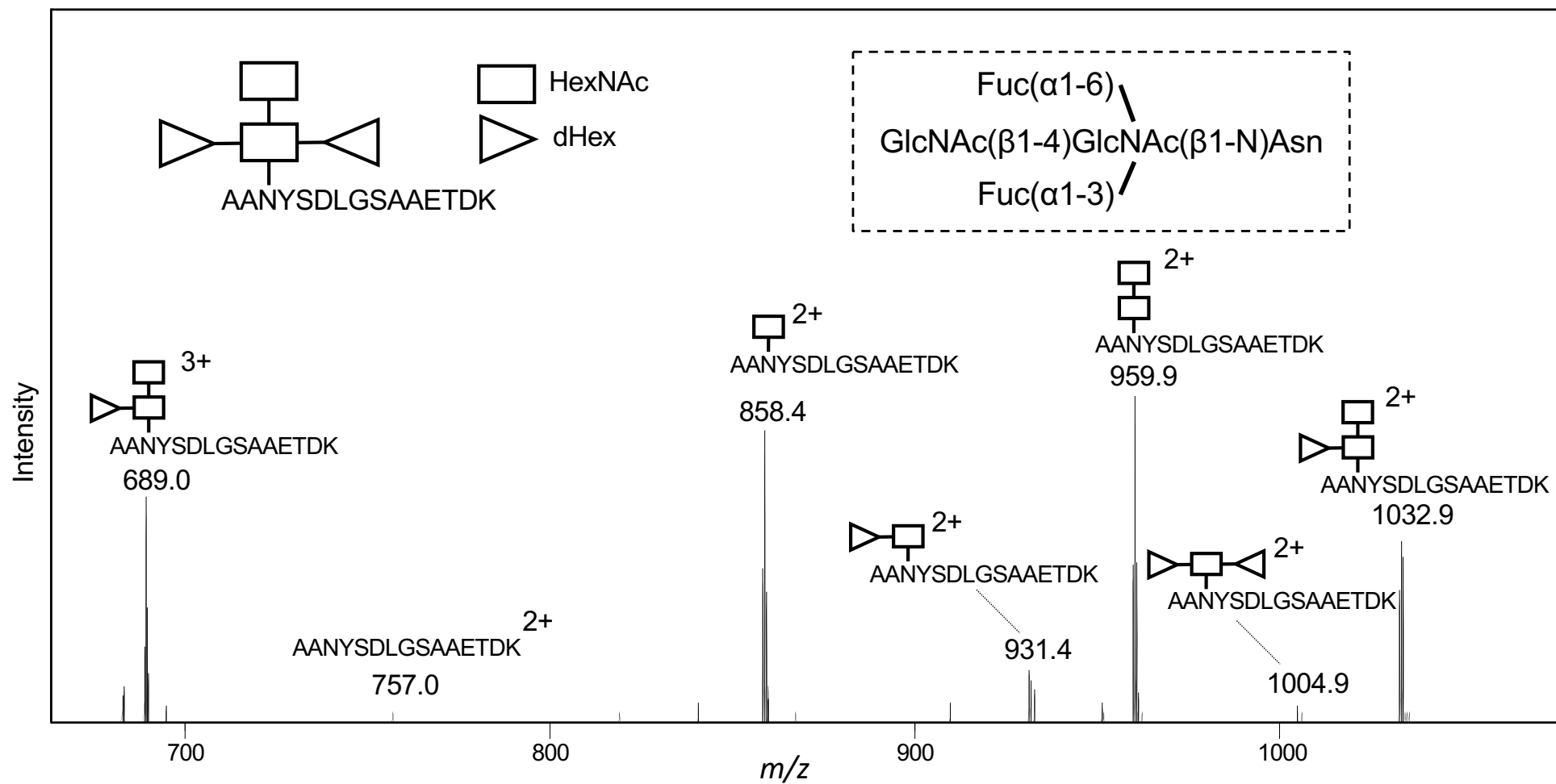


Figure 8. Product ion spectrum of the Lys-C digest containing N-glycosylation and its estimated glycan structure (dashed square).

```

LaPLA2-1      MVFIFLAVLSGLVTLSSHSTAVQREMHHVHFEPLPGQRDSWPVARAALVNLATKSETGRE--
Hemilipin     MTFILILTILATVTPSLYSHVVQRELRVNFEPLAGQRDSWPVARAAMVTFDARSEKARE--
HgPLA2       MSLIIVLVISVL---SADAVLSMDNELYLNLPEPSQRSSWPVARAVRMQFSKRSEGGRESR
Phaiodactylipin -----
BvPLA2

LaPLA2-1      -FSDCRMNSIDEIAREGAVLSRYEIKRVSKEEMRSLEKRCRSRSSGIHQRLIFPGTKWCG
Hemilipin     -FSECRMINSMHELSRELMDSPHPTVKRASKEEMDDLVRCSGSAEGRSWFIWPDTKWCG
HgPLA2       KMQGCQILESLNDIAREALRTPRHSTTKRISKDEMEFFEGRCLSVGSESE--TVLGTKWCG
Phaiodactylipin -----MVKRVSKKEEMDALERSCSQPFEERFLIVSGTKWCG
BvPLA2       -----MQVVLGSLFLLLL-----S-TSHGWQIRDRIGDNELEERLIYPGTLWCG

LaPLA2-1      vv
Hemilipin     AGDKAANYSDLGSAAE▲TDKCCRAHDH▲CDN-IAAGETKYGLENSYWFTKLNCKCEESFRNC
HgPLA2       PGTDAKNESDLGPF-LEADKCCRTHDH▲CDY-IGAGETKYGLTNKSF▲FTKLNCKCEAAF▲DQC
Phaiodactylipin -----AGNEAANYSDLGYFNNVDRCCREHDH▲CDN-IPAGETKYGLKNEGTYTMMNCKCEKAF▲DKC
BvPLA2       NNNIAANYSDLGF-LEADKCCRDHDH▲CDH-IAAGETKYGLENKGLFTILNCKCEAF▲DHC
HgPLA2       HCNKSSGPNELGRFKHTDA▲CCRTHDM▲CPDVMSAGESKHKGLTNTASHTRLSCD▲DDKFYDC

LaPLA2-1      LAEAKKKT-----TAKFVKFSYFNVYGPKC▲FVLD▲DKRRFEM--SRK-----
Hemilipin     LKESIDRAEGS--AKSSMEGLHSFYFNTYSPEC▲YEVK▲CSRKRDAE--CTN-----
HgPLA2       LSDISGYFTRK-----AVSAVKFTYFTLYGNGC▲YNVK▲CENGRSPSNE▲CPN-----
Phaiodactylipin -----LKEISNVTTDIRQKGAENVWRFYFQWYNAN▲CYRLY▲CKDEKSAR--DEA-----
BvPLA2       LKNSADTIS-----SYFVGRMYFNLDITKC▲YKLEHPVTG▲GERTEGR▲CLHYTVDKSK

LaPLA2-1      -CAHHWKESRRG-----100 (%Id)
Hemilipin     -GIAIWKDSYK-----49
HgPLA2       -GVAEYTG▲ETG=LGAKVINFGK41
Phaiodactylipin -----CTNQYAVVKKNFTVQ-----46
BvPLA2       PKVYQWF▲DLRKY-----26

```

Figure 9. Multiple sequence alignment of LaPLA<sub>2</sub>-1 and its related PLA<sub>2</sub> molecules. Mature regions that were experimentally determined are underlined. Cys residues in the mature regions are shaded in yellow. Open triangles indicate the Ca<sup>2+</sup>-binding motif. Closed triangles indicate the catalytic dyad. N-glycosylation motif is shown in bold. The N-glycosylation sites that were experimentally confirmed are shown in red. %Id represents the percentage of sequence identity.



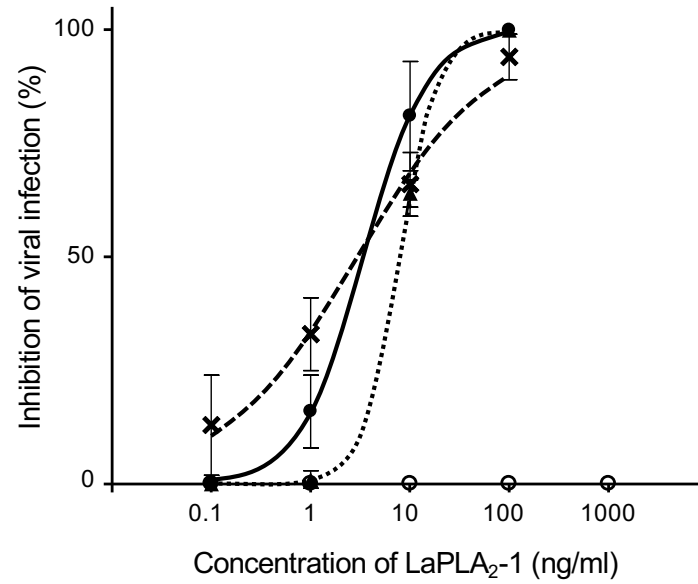


Figure 10 Representative concentration-inhibition curves for LaPLA<sub>2</sub>-1 on HCV (●), DENV (×), JEV (▲), and HSV-1 (○) infection. Each point represents means ± SEM.

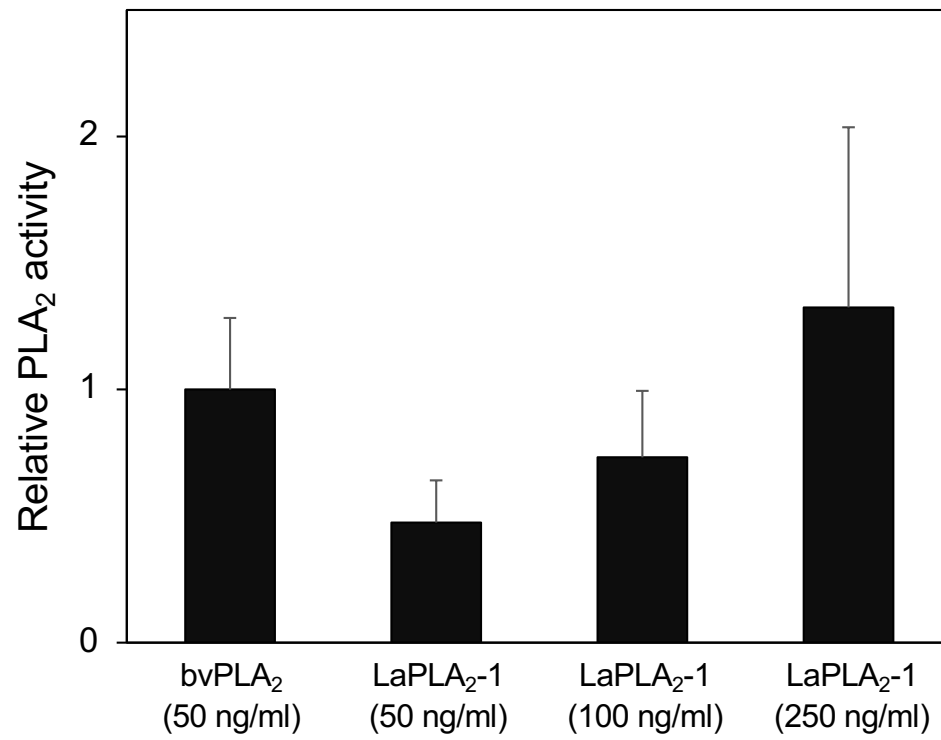


Figure 11. Comparison of PLA<sub>2</sub> activity between bvPLA<sub>2</sub> and LaPLA<sub>2</sub>-1

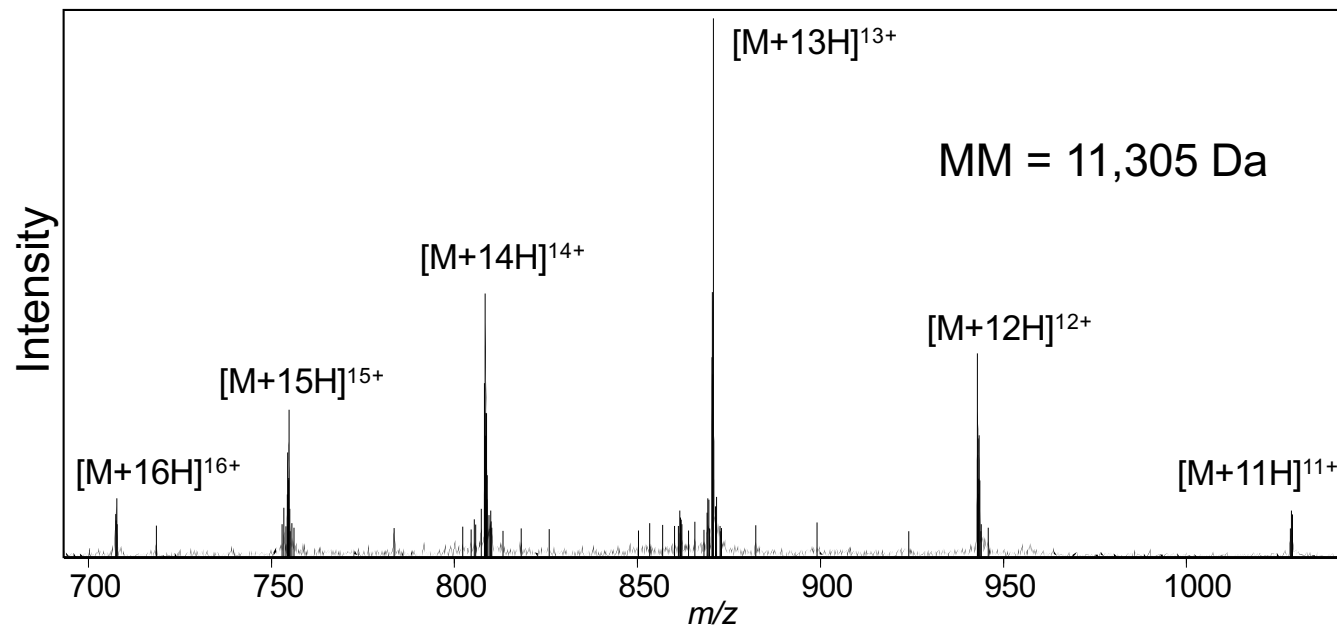


Figure S1 Mass spectrum of LaPLA<sub>2</sub>-1 after deglycosylation